

Manuscript prepared for Geosci. Model Dev.  
with version 2014/09/16 7.15 Copernicus papers of the L<sup>A</sup>T<sub>E</sub>X class copernicus.cls.  
Date: 22 May 2015

# Addressing the Challenge of Nonnegativity in Coupling a Reactive Transport Code with a Global Land Surface Model for Mechanistic Biogeochemistry Representation

Guoping Tang<sup>1</sup>, Fengming Yuan<sup>1</sup>, Gautam Bisht<sup>1,2</sup>, Glenn E. Hammond<sup>3</sup>, Peter C. Lichtner<sup>4</sup>, Nathaniel, O. Collier<sup>1</sup>, Jitu Kumar<sup>1</sup>, Xiaofeng Xu<sup>1,6</sup>, Richard T. Mills<sup>1,5</sup>, Forrest M. Hoffman<sup>1</sup>, Scott L. Painter<sup>1</sup>, and Peter E. Thornton<sup>1</sup>

<sup>1</sup>Oak Ridge National Laboratory, Oak Ridge, Tennessee, United States

<sup>2</sup>Lawrence Berkeley National Laboratory, Berkeley, California, United States

<sup>3</sup>Sandia National Laboratories, Albuquerque, New Mexico, United States

<sup>4</sup>OFM Research, Redmond, Washington, United States

<sup>5</sup>Intel Incorporation, Portland, Oregon, United States

<sup>6</sup>University of Texas at El Paso, El Paso, Texas, United States

*Correspondence to:* NAME (EMAIL)

This manuscript has been authored by UT-Battelle, LLC under Contract No. DE-AC05-00OR22725 with the U.S. Department of Energy. The United States Government retains and the publisher, by accepting the article for publication, acknowledges that the United States Government retains a non-exclusive, paid-up, irrevocable, world-wide license to publish or reproduce the published form of this manuscript, or allow others to do so, for United States Government purposes. The Department of Energy will provide public access to these results of federally sponsored research in accordance with the DOE Public Access Plan(<http://energy.gov/downloads/doe-public-access-plan>).

**Abstract.** Reactive transport codes (e.g., PFLOTTRAN) are increasingly used to improve the representation of biogeochemical processes in terrestrial ecosystem models (e.g., the Community Land Model, CLM). As CLM and PFLOTTRAN use explicit and implicit time stepping, implementation of CLM biogeochemical reactions in PFLOTTRAN can result in negative concentration, which is not physical and can cause numerical instability and errors. The objective of this work is to implement CLM subsurface biogeochemical reactions in CLM-PFLOTTRAN with a focus on addressing the non-negativity challenge to obtain accurate, efficient, and robust solutions. We implement the CLM-CN decomposition, nitrification, denitrification, and plant nitrogen uptake reactions and test the implementation at arctic, temperate, and tropical sites. We examine use of scaling back the update during each iteration (SU), log transformation (LT), and downregulating the reaction rate to account for reactant availability limitation to enforce nonnegativity. Both SU and LT guarantee nonnegativity but with implications. When a very small scaling factor occurs due to either consumption or numerical overshoot, and the iterations are deemed converged because of too small an update, SU can introduce excessive numerical error. LT involves multiplication of the Jacobian matrix by the concentration vector, which increases the condition number, decreases the time step size, and increases the computational cost. Neither SU nor SE prevents zero concentration. When the concentration is close to machine precision or 0, a small positive update stops all reactions for SU, and LT can fail due to a singular Jacobian matrix. The consumption rate has to be downregulated such that the solution to the mathematical representation is positive. A first-order rate downregulates consumption and is nonnegative, and adding a residual concentration makes it positive. For zero-order rate or when the reaction rate is not a function of a reactant, representing the availability limitation of each reactant with a Monod substrate limiting function provides a smooth transition between a zero-order rate when the reactant is abundant and first-order rate when the reactant becomes limiting. Marching through the transition may require small time step sizes when the half saturation is small. Our results from simple tests and CLM-PFLOTTRAN simulations caution against use of SU and indicate that accurate, stable, and relatively efficient solutions can be achieved with LT and downregulation with Monod substrate limiting function and residual concentration.

35 **1 Introduction**

Methods developed for the reactive transport models (??) and geochemical codes (??) are increasingly used to improve the representation of biogeochemical processes in terrestrial ecosystem models (TEMs, e.g., the Community Land Model, CLM) for better climate prediction. An essential aspect of these TEMs is the ability to simulate competition for nutrients (e.g., mineral nitrogen, 40 phosphate, etc.) among plants and microbes. For example, the CLM-CN decomposition cascade downregulates the demand based on the available nitrogen (N) (??). Specifically, marching from time step  $k$  to  $k+1$  with a supply rate  $S^k$  and consumption rate  $D^k$  using the forward difference,  $[N]^{k+1} = [N]^k + (S^k - D^k)\Delta t$ . ( $[ ]$  is used to denote concentration.) CLM replaces  $D^k$  with  $\min(D^k, [N]^k/\Delta t)$  so that  $[N]^{k+1} \geq S^k\Delta t \geq 0$ . As a result,  $[N]$  is nonnegative in CLM.

45 Geochemical codes generally use implicit time stepping such as the backward difference,  $([N]^{k+1} - [N]^k)/\Delta t = S^{k+1} - D^{k+1}$ . Solving this nonlinear equation with the Newton-Raphson method to iterate from  $p$  to  $p+1$ ,

$$[N]^{k+1,p+1} = [N]^{k+1,p} - \frac{\frac{[N]^{k+1,p} - [N]^k}{\Delta t} - S^{k+1,p} + D^{k+1,p}}{\frac{1}{\Delta t} - \frac{\partial S^{k+1,p}}{\partial [N]^{k+1,p}} + \frac{\partial D^{k+1,p}}{\partial [N]^{k+1,p}}} \quad (1)$$

Depending on  $[N]^k$ ,  $\Delta t$ ,  $S^{k+1,p}$ ,  $D^{k+1,p}$ , and the derivatives,  $[N]^{k+1,p+1}$  can be negative, which is 50 not physical, and can cause numerical instability and errors (?).

Enforcing nonnegativity is a common challenge in science, engineering, and business, including, for example, image processing, optimization, and ecosystem and geochemical modeling (?????????). The challenge increases in geochemical modeling because the concentration can be very low. For example, the threshold concentration for  $H_2$  is 1.5 nM ( $10^{-9}M$ ) for dechlorinators and 5~20 nM 55 for methanogens (?). The EPA maximum contaminant level for drinking water for dioxin is 30 ppq ( $3.5 \times 10^{-13} M$ ). The redox potential Eh needs to be decreased to  $-0.35 V$  (corresponding to an  $O_2$  concentration  $< 10^{-22} M$  ?, ?) for methanogens to grow (?). With very low concentration, a small consumption or numerical oscillation can lead to negative concentration.

Two methods are used to avoid negative concentration in geochemical codes. One is to use the 60 logarithm concentration as the primary variable (??). Log transformation (LT) is well suited for solving the mass action equations because it converts these nonlinear equations into linear equations. However, LT converts linear advection and diffusion equations into nonlinear equations, which may increase the computational cost (?). The other approach (SU) scales back the update in each of the Newton-Raphson iteration to enforce nonnegativity (??). Both methods are available in PFLO- 65 TRAN and some other geochemical codes (e.g., Geochemist's Workbench, ?, ?). However, to our knowledge, the implications of these approaches have not been thoroughly examined, particularly for application to CLM.

Competition for nutrients (for instance, labile carbon, phosphate,  $O_2$ , and  $H_2$ ) is common in 70 terrestrial ecosystems, and is increasingly incorporated in process-rich models. As the terrestrial

70 ecosystem models are often run under a variety of conditions around the globe for hundreds of years  
 with a time step as small as half an hour, proper treatment of the nonnegativity issue is necessary  
 for accurate, efficient, and robust simulation of biogeochemical processes using reactive transport  
 codes for earth system models. The objective of this work is to implement CLM subsurface biogeo-  
 chemical reactions in CLM-PFLOTRAN with the focus on addressing the nonnegativity challenge  
 75 to obtain accurate, efficient, and robust solutions. We implement the CLM-CN decomposition (??);  
 nitrification; denitrification (??); and plant nitrogen uptake reactions in CLM-PFLOTRAN and test  
 the implementation at arctic, temperate, and tropical sites. In addition to SU and LT that are avail-  
 able in PFLOTRAN, we examine ways to downregulate consumption to account for the limitation  
 of reactant availability on reaction rate. While this work focuses on addressing the nonnegativity  
 80 challenge for biogeochemistry, detailed comparison of the results of CLM and CLM-PFLOTRAN  
 biogeochemistry representation and comprehensive CLM-PFLOTRAN coupling in heat transfer (in-  
 cluding freeze and thaw), hydrology, and biogeochemistry will be presented in future publications.  
 While we use CLM-PFLOTRAN to implement and test simple carbon and nitrogen reactions at a  
 few sites, we hope that what we develop here will be relevant for a wide range of applications.

## 85 2 Biogeochemistry

### 2.1 CLM biogeochemistry

The terrestrial ecosystem models generally include biogeochemical reactions for carbon and nitro-  
 gen cycles, in particular, the organic matter decomposition, nitrification, dentrification and methane  
 production and oxidation. The kinetics are usually described by a first-order rate modified by re-  
 90 sponse functions for environmental variables (temperature, moisture, pH, etc.) (??). In this work,  
 we use the CLM-CN decomposition (??), nitrification, denitrification (??), and plant nitrogen  
 uptake reactions (Fig. 1) as an example.

#### 2.1.1 CLM-CN decomposition

The CLM-CN decomposition cascade consists of three litter pools with variable CN ratios, four soil  
 95 organic matter (SOM) pools with constant CN ratios, and seven reactions (Fig. 1A). The reaction  
 can be described by

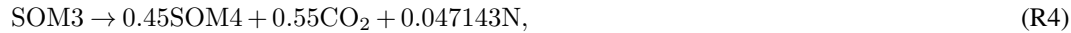
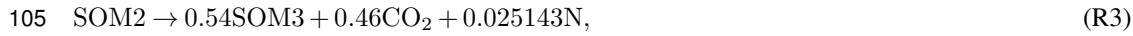
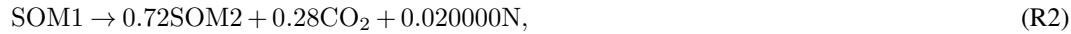


with  $\text{CN}_u$  and  $\text{CN}_d$  as the upstream and downstream pool (molecular formula), N as either  $\text{NH}_4^+$  or  
 $\text{NO}_3^-$ ,  $f$  as the respiration fraction, and  $n = u - (1 - f)d$ . The rate is

$$100 \quad \frac{\partial[\text{CN}_u]}{\partial t} = -k_d f_T f_w [\text{CN}_u], \quad (2)$$

with  $k_d$  as the rate coefficient and  $f_T$  and  $f_w$  as the temperature and moisture response functions.

With a constant CN ratio, the decomposition reactions for the four SOM pools are



and

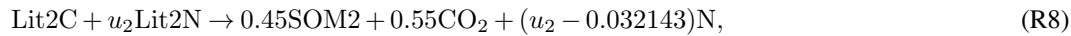
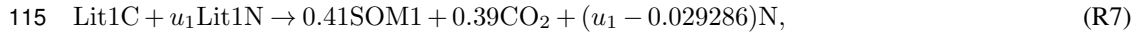


110 CLM4.5 has an option to separate N into  $\text{NH}_4^+$  and  $\text{NO}_3^-$ . The N mineralization product is  $\text{NH}_4^+$ .

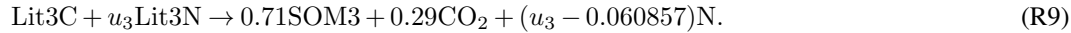
As the CN ratio is variable for the three litter pools, litter N pools need to be tracked such that reaction (R1) becomes



with  $u = [\text{LitN}]/[\text{LitC}]$ . The three litter decomposition reactions are



and



120 As the CN ratio of the litter pools is generally high,  $u_1$ ,  $u_2$ , and  $u_3$  are usually small, and  $n$  in these reactions (e.g.,  $n_1 = u_1 - 0.029286$  for Lit1) is normally negative. Namely, these reactions consume (immobilize) N, which can be  $\text{NH}_4^+$ ,  $\text{NO}_3^-$ , or both.

## 2.1.2 Nitrification

The nitrification reaction to produce  $\text{NO}_3^-$  is



with rate (Dickinson et al., 2002)

$$\frac{\partial[\text{NH}_4^+]}{\partial t} = -\frac{\partial[\text{NO}_3^-]}{\partial t} = -k_n f_T f_w [\text{NH}_4^+]. \quad (3)$$

The nitrification reaction to produce N<sub>2</sub>O is



130 with one component related to decomposition as

$$\frac{\partial[\text{NH}_4^+]}{\partial t} = -2 \frac{\partial[\text{N}_2\text{O}]}{\partial t} = -f_{\text{nm}} f_T f_w f_{\text{pH}} \max(R_{\text{nm}}, 0) \quad (4)$$

with  $f_{\text{nm}}$  as a fraction (?) and  $R_{\text{nm}}$  as the net N mineralization rate,

$$R_{\text{nm}} = \sum_i n_i R_i, \quad (5)$$

where  $R_i$  denotes the rate of reaction (R2, R3, R4, R5, R7, R8, R9). The second component is (?)

$$135 \quad \frac{\partial[\text{NH}_4^+]}{\partial t} = -2 \frac{\partial[\text{N}_2\text{O}]}{\partial t} = -k_{\text{n2o}} f_T f_w f_{\text{pH}} (1 - e^{-0.0105[\text{NH}_4^+]}) . \quad (6)$$

Ignoring the high-order terms and moving the unit conversion factor into  $k_{\text{n2o}}$ , it can be simplified as a first-order rate as

$$\frac{\partial[\text{NH}_4^+]}{\partial t} = -2 \frac{\partial[\text{N}_2\text{O}]}{\partial t} = -k_{\text{n2o}} f_T f_w f_{\text{pH}} [\text{NH}_4^+]. \quad (7)$$

### 2.1.3 Denitrification

140 The denitrification reaction is



with rate (?)

$$\frac{\partial[\text{NO}_3^-]}{\partial t} = -2 \frac{\partial[\text{N}_2]}{\partial t} = -k_{\text{deni}} f_T f_w f_{\text{pH}} [\text{NO}_3^-]. \quad (8)$$

### 2.1.4 Plant nitrogen uptake

145 The plant nitrogen uptake reaction can be written as



and



The rate is specified by CLM (plant nitrogen demand) and assumed to be constant in each half-hour

150 time step.

### 2.1.5 Demand-based competition and distributing nitrogen demand between $\text{NH}_4^+$ and $\text{NO}_3^-$

Denote  $R_{d,p}$ ,  $R_{d,i}$ ,  $R_{d,nitr}$ ,  $R_{d,deni}$  as the potential plant, immobilization, nitrification, and denitrification demand (rate);  $R_{a,tot} = R_{d,p} + R_{d,i} + R_{d,nitr}$  as the total  $\text{NH}_4^+$  demand; and  $R_{n,tot}$  as the total  $\text{NO}_3^-$  demand. CLM uses a demand-based competition approach to split the available sources in proportion to the demand rates to meet the demands (??). Specifically, for each time step, if  $R_{a,tot}\Delta t \leq [\text{NH}_4^+]$ , the uptakes are equal to potential demands, and  $R_{n,tot} = 0$ ; otherwise, the uptakes for  $\text{NH}_4^+$  are  $[\text{NH}_4^+]R_{d,p}/R_{a,tot}\Delta t$ ,  $[\text{NH}_4^+]R_{d,i}/R_{a,tot}\Delta t$ , and  $[\text{NH}_4^+]R_{d,nitr}/R_{a,tot}\Delta t$  for plants, immobilization, and nitrification, respectively;  $R_{n,tot} = R_{a,tot} - [\text{NH}_4^+]/\Delta t + R_{d,deni}$ . If  $R_{n,tot}\Delta t < [\text{NO}_3^-]$ , all of the remaining demand  $R_{n,tot}$  is met with available  $\text{NO}_3^-$ . Otherwise, available  $\text{NO}_3^-$  is split to meet the remaining plant, immobilization, and denitrification demands in proportion to their rates.

## 2.2 CLM-PFLOTRAN biogeochemistry

In CLM-PFLOTRAN, CLM instructs PFLOTRAN to solve the partial differential equations for energy (including freezing and thawing), water flow, and reaction and transport in the surface and subsurface. This work focuses on the biogeochemistry (energy, hydrology and overall coupling will be described in future publications). Specifically, we focus on addressing the nonnegativity challenge for the geochemical reactions, with CLM solving the energy and water flow equations and handling the solute transport (mixing, advection, diffusion, and leaching).

In each time step, CLM provides production rates for Lit1C, Lit1N, Lit2C, Lit2N, Lit3C, Lit3N for litter fall;  $\text{NH}_4^+$  and  $\text{NO}_3^-$  for nitrogen deposition and fixation; and plant N demand (rate); and specifies liquid water content, matrix potential and temperature for PFLOTRAN; PFLOTRAN solves the ordinary differential equations for the kinetic reactions and provides the final concentrations back to CLM.

PFLOTRAN does not track individual reaction rates such as total nitrogen mineralization rate. We add hypothetical species (diagnostic variables), e.g., PlantN, N2Od, and DeniN, to track  $\text{NO}_3^-$  uptake by plants as in reaction (R14);  $\text{N}_2\text{O}$  production from nitrification reaction (R11) due to net mineralization (Eq. 4); and denitrification (R12). At the end of each time step, CLM uses the change of these concentration to calculate the specific rates. To simplify the calculations, we reset these concentrations to  $10^{-10}$  at the beginning of each time step instead of storing the values of the previous time step.

The reactions and rates such as those described in Section 2.1 are implemented using the “reaction sandbox” concept in PFLOTRAN (?). For each reaction, we specify a rate and a derivative of the rate with respect to any components in the rate formula, given concentrations, temperature, moisture content, grid cell volume, and other environmental variables. PFLOTRAN accumulates these rates and derivatives into a residual vector and a Jacobian matrix, and the global equation is discretized in

time using the backward difference and solved using the Newton-Raphson method. Ignoring equilibrium reactions and transport for simplicity of discussion in this work, PFLOTRAN solves the ordinary differential equation,

$$\frac{\partial \mathbf{c}}{\partial t} = \mathbf{R}(\mathbf{c}), \quad (9)$$

- 190 with  $\mathbf{c}$  as the concentration vector and  $\mathbf{R}$  as the kinetic reaction rate. Discretizing Eq. (9) in time using the backward difference,

$$\frac{\mathbf{c}^{k+1} - \mathbf{c}^k}{\Delta t} = \mathbf{R}(\mathbf{c}^{k+1}). \quad (10)$$

Solving the equation using the Newton-Raphson method,

$$\mathbf{f}(\mathbf{c}^{k+1,p}) = (\mathbf{c}^{k+1,p} - \mathbf{c}^k)/\Delta t - \mathbf{R}(\mathbf{c}^{k+1,p}), \quad (11)$$

195

$$\mathbf{J} = \frac{\partial \mathbf{f}(\mathbf{c}^{k+1,p})}{\partial \mathbf{c}^{k+1,p}}, \quad (12)$$

$$\delta \mathbf{c}^{k+1,p} = \mathbf{J}^{-1} \mathbf{f}(\mathbf{c}^{k+1,p}), \quad (13)$$

and

$$200 \quad \mathbf{c}^{k+1,p+1} = \mathbf{c}^{k+1,p} - \delta \mathbf{c}^{k+1,p}. \quad (14)$$

The iteration continues until either the residual  $\mathbf{f}(\mathbf{c}^{k+1,p})$  or the update  $\delta \mathbf{c}^{k+1,p}$  is less than a specified tolerance. Specifically,

$$||\mathbf{f}(\mathbf{c}^{k+1,p})||_2 < \text{ATOL}, \quad (15)$$

$$205 \quad \frac{||\mathbf{f}(\mathbf{c}^{k+1,p})||_2}{||\mathbf{f}(\mathbf{c}^{k+1,0})||_2} < \text{RTOL}, \quad (16)$$

$$\frac{||\delta \mathbf{c}^{k+1,p}||_2}{||\mathbf{c}^{k+1,p}||_2} < \text{STOL}, \quad (17)$$

$$||\mathbf{f}(\mathbf{c}^{k+1,p})||_\infty < \text{ITOL\_RES}, \quad (18)$$

210 and

$$||\delta \mathbf{c}^{k+1,p}||_\infty < \text{ITOL\_UPDATE}. \quad (19)$$

If none of these tolerances are met in MAXIT iterations or MAXF function evaluations, the iteration is considered to diverge, and PFLOTRAN decreases the time step size for MAX\_CUT times. The default values in PFLOTRAN are ATOL =  $10^{-50}$ , RTOL =  $10^{-8}$ , STOL =  $10^{-8}$ , ITOL\_RES =  
215 ITOL\_UPDATE =  $10^{-50}$ , MAXIT = 50, MAXF =  $10^4$ , and MAX\_CUT = 16.

Unlike the explicit time stepping in CLM for biogeochemistry where only the reaction rates need to be calculated, the implicit time stepping used in PFLOTRAN and other geochemical codes requires the derivatives. While PFLOTRAN provides the option to calculate the Jacobian numerically, geochemical codes generally prefer analytical Jacobian calculation (e.g., ?) because numerical calculation for accurate Jacobian approximation is a notoriously difficult task (?). Many reactions can be specified, and the rates and derivatives are accumulated in the residual and Jacobian, providing flexibility in specifying various reactions with a user-defined rate formula. In contrast, the number of pools and reactions were traditionally hard-coded in CLM. Therefore, this new approach facilitates implementation of increasingly mechanistic reactions and tests of various representations without  
220 code modifications.  
225

### 3 Approaches

Like Eq. (1), one of the basic challenges for using geochemical code for CLM is that Eq. (14) is not guaranteed to be positive. Both SU (scaling back the update during each iteration) and LT (log transformation) are available in PFLOTRAN to enforce nonnegativity. However, to our knowledge,  
230 the limitations and implications of both methods have not been thoroughly examined.

#### 3.1 Scaling back update in iterations

SU scales back the update (Eq. 14) with a scaling factor  $\lambda$  (??) such that

$$\mathbf{c}^{k+1,p+1} = \mathbf{c}^{k+1,p} - \lambda \delta \mathbf{c}^{k+1,p} > 0, \quad (20)$$

where

$$235 \quad \lambda = \alpha \min \left[ 1, \frac{\mathbf{c}^{k+1,p}(i)}{\delta \mathbf{c}^{k+1,p}(i)} \right] \quad (21)$$

for positive  $\delta \mathbf{c}^{k+1,p}(i)$  and  $i = 1$  to  $m$ , with  $m$  as the number of species times the number of numerical grid cells. With SU, the concentration of the species that is going negative decreases by  $(1 - \alpha)$  times in each iteration instead. This can be shown by solving the zero-order uptake problem  $dc/dt = -1$ :  $c^{k+1} = c^k - \Delta t$  when  $\Delta t \geq c^k$ ; otherwise,  $\lambda = \alpha c^k / \Delta t$ , and  $c^{k+1} = (1 - \alpha)c^k$ .  
240 With a default  $\alpha = 0.99$  in PFLOTRAN, each iteration reduces the concentration by 100 times. With multiple iterations, the concentration can approach machine precision or 0.

The choice of  $\alpha$  and the value of  $\lambda$  are expected to influence the convergence process and may introduce numerical error under certain conditions. For example, if  $\mathbf{c}^{k+1,p}(i)$  is 0 (or below the

machine precision), and  $\delta\mathbf{c}^{k+1,p}(i) > 0$ , then  $\lambda = 0$ , and the update is limited to 0 and the residual  
245 will not be decreased to satisfy Eqs. (15 or 16) to achieve convergence. If the iteration is deemed converged because the scaled update is 0, and Eq. (17) is met, the calculation will march through this time step without any change in the concentrations, numerically stopping all reactions. This can continue for many time steps until  $\delta\mathbf{c}^{k+1,p}(i)$  becomes negative.

Application of a very small scaling factor  $\lambda$  due to decrease of a small concentration for one  
250 species may have a similar consequence: the iteration may not decrease the residual  $\mathbf{f}(\mathbf{c}^{k+1,p})$  or the iteration may not converge because Eqs. (15 or 16) are not met. If the iteration is considered converged because of too small an update  $\lambda\delta\mathbf{c}^{k+1,p}$  (Eq. 17 is satisfied), the scaling factor  $\lambda$  (e.g.,  $10^{-10}$ ) may correctly limit the consumption reaction rates to account for availability limitation, but wrongfully limit the production rate in the time step. This can be illustrated by adding to the zero-order  
255 uptake problem  $dc/dt = -1$  an independent zero order production  $de/dt = 1$ : when  $\Delta t \geq c^k$ ,  $\lambda = \alpha c^k / \Delta t$ ,  $c^{k+1} = (1 - \alpha)c^k$ ,  $e^{k+1} = e^k + \alpha c^k$  rather than  $e^{k+1} = e^k + \Delta t$ . If  $c^k = 0$ , SU numerically stops the independent production reaction.

To avoid excessive numerical error, PFLOTTRAN reports an error and exits when  $\lambda < \lambda_{\min}$ , with a default  $\lambda_{\min} = 10^{-10}$ . This translates the accuracy issue into a stability issue. It is necessary to  
260 investigate SU to resolve both the accuracy issue and the stability issue.

### 3.2 Log transformation

LT is widely used in geochemical codes to enforce positivity (???). Instead of solving Eq. (11) for  $\mathbf{c}^{k+1}$  using Eqs. (12,13,14), LT solves for  $(\ln \mathbf{c}^{k+1})$  from

$$\mathbf{J}_{\ln}(i,j) = \frac{\partial \mathbf{f}(i)}{\partial \ln(\mathbf{c}(j))} = \mathbf{c}(j) \frac{\partial \mathbf{f}(i)}{\partial \mathbf{c}(j)} = \mathbf{J}(i,j), \quad (22)$$

265

$$\delta \ln \mathbf{c}^{k+1,p} = \mathbf{J}_{\ln}^{-1} \mathbf{f}(\mathbf{c}^{k+1,p}), \quad (23)$$

and

$$\mathbf{c}^{k+1,p+1} = \mathbf{c}^{k+1,p} \exp[-\delta \ln(\mathbf{c}^{k+1,p})]. \quad (24)$$

One downside is apparent from Eq. (22): suppose  $\mathbf{c}^{k+1,p}(j) = 10^{-10}$ ;  $\mathbf{J}(i,j)$  (column  $j$  of the Jacobian) decreases by  $10^{10}$  times to  $\mathbf{J}_{\ln}(i,j)$ . As a result, the condition number of the Jacobian matrix may increase by orders of magnitudes, which may constrain the time step size to be substantially reduced, comparing to the case without LT. Secondly, the small eigenvalues may result in large  $\delta \ln \mathbf{c}^{k+1,p}$ , which may cause overshooting to an unrealistically large concentration (positive update), or essentially 0 concentration (negative update), or even overflow in the exponential function in Eq.  
275 (24). To prevent these problems, PFLOTTRAN limits the update to

$$\delta \ln(\mathbf{c}^{k+1,p}) = \text{sign}[\delta \ln(\mathbf{c}^{k+1,p})] \min[\text{abs}(\delta \ln \mathbf{c}^{k+1,p}), \delta_{\ln, \max}] \quad (25)$$

with a default  $\delta_{\ln,\max} = 5$ . Thirdly, LT does not prevent 0 concentration per se: a number of iterations with positive  $\delta \ln \mathbf{c}^{k+1,p}(j)$  update is likely to bring  $\mathbf{c}^{k+1,p+1}(j)$  to be below machine precision or 0. With zero concentration,  $\mathbf{J}_{\ln}$  becomes singular, and the numerical solution fails. These can be shown by solving  $dc/dt = -1$  in the log transformed form  $d \ln c/dt = -1/c$ :  $c^{k+1} = c^k e^{-\Delta t/c^{k+1}}$ . LT converts the linear problem that does not require iteration to a nonlinear problem that needs to be solved iteratively. As  $c^{k+1}$  becomes small,  $\Delta t$  has to be decreased accordingly, or the concentration goes to below machine precision and a  $c^{k+1} = 0$  causes division by 0 overflow.

### 3.3 Downregulation of reaction rate

Even though ensuring nonnegativity, the concentrations can become very small or essentially 0 using either SU or LT. With 0 or near 0 concentrations, the scaling factor for SU is small or 0, or the time step sizes for LT are too small if LT does not fail due to a singular Jacobian matrix. Both approaches require the solution to the mathematical representation itself be positive. To obtain such a mathematical representation, it is necessary to downregulate reaction rates to represent the limitation of the availability of each reactant on the reaction rate. In the geochemical modeling literature, this is mostly represented by a rate limiting function as a function of concentration in each reaction for each reactant. CLM downregulates demand (consumption) as a function of rate (demand-based competition). We examine downregulation of consumption as a function of concentration (DC) and rate (DR) for use with SU or LT to address the nonnegativity challenge.

#### 3.3.1 Downregulation of consumption as a function of concentration

The first-order decay problem (Eqs. 2, 3, 6, 8) is nonnegative. This can be shown by solving the first-order problem  $dc/dt = -c$  using the backward difference:  $c^{k+1} = c^k/(1 + \Delta t)$ ; the concentration decreases but remains nonnegative. However, it can go to 0. To avoid 0 concentration, a residual term is often used to limit the decay to a residual concentration (?). For example, Eq. (2) becomes

$$300 \quad \frac{\partial [\text{CN}_u]}{\partial t} = -k_d f_T f_w ([\text{CN}_u] - [\text{CN}_u]_r). \quad (26)$$

When the concentration goes below  $[\text{CN}_u]_r$  (overshoots) in an iteration, Eq. (26) implies a hypothetical reverse reaction to bring it back to  $[\text{CN}_u]_r$ . An alternative is to introduce a cutoff, e.g., Eq. (2) becomes

$$\frac{\partial [\text{CN}_u]}{\partial t} = -k_d f_T f_w [\text{CN}_u] f([\text{CN}_u]), \quad (27)$$

305 with  $f([\text{CN}_u]) = 1$  when  $[\text{CN}_u] \geq [\text{CN}_u]_r$ , and 0 otherwise. It is simple but does not prevent  $[\text{CN}_u]$  from getting below  $[\text{CN}_u]_r$  or 0 in theory. In addition, it introduces a discontinuity. A polynomial function can be used to smooth the cutoff

$$f([\text{CN}_u]) = 1 - \left[ 1 - \left( \frac{[\text{CN}_u] - [\text{CN}_u]_r}{[\text{CN}_u]_1 - [\text{CN}_u]_r} \right)^2 \right]^2. \quad (28)$$

This function varies from 0 at  $[CN_u]_r$  to 1 at  $[CN_u]_1$ , with zero derivatives at both points. While  
 310 not implying a nonphysical reverse reaction as Eq. (26),

$$\frac{df([CN_u])}{d[CN_u]} = 4 \frac{[CN_u] - [CN_u]_r}{([CN_u]_1 - [CN_u]_r)^2} \left[ 1 - \left( \frac{[CN_u] - [CN_u]_r}{[CN_u]_1 - [CN_u]_r} \right)^2 \right]. \quad (29)$$

Depending on  $[CN_u]_1 - [CN_u]_r$ , this cutoff does introduce a large derivative change during the transition:  $df([CN_u])/d[CN_u]$  varies from 0 to  $10^8$  for  $[CN_u]_r=10^{-10}$  and  $[CN_u]_1=10^{-8}$  (Fig. 2). The maximum increases at about the same order of magnitude as the decrease of  $[CN_u]_r$  and  
 315  $[CN_u]_1$ . Even though smoothed, the cutoff is still a sharp change. The smaller the cutoff concentrations, the sharper the transitions. Marching through a steep transition in time usually involves small time steps. In contrast, the residual concentration introduced in Eq. (26) does not adjust the derivative, which appears less nonlinear. Obviously, enforcing positivity even for a linear problem (here the first-order rate) introduces nonlinearity into the numerical problem. A smaller threshold may  
 320 lead to higher nonlinearity. For example, even though a  $NO_3^-$  concentration of  $10^{-10}$  M may not be detectable, and is not any different from  $10^{-15}$  M, introducing the cutoff of Eq. (28) with a cutoff  $10^{-15}$  produces five orders of magnitude more increase in the derivative than a cutoff of  $10^{-10}$ . In the case when extremely low concentration matters (e.g.,  $O_2$ ), enforcing positivity with the implicit time stepping and Newton-Raphson method is numerically challenging.

325 For the litter decomposition reactions (R7, R8, R9) that immobilize nitrogen, the rate formulae (Eqs. 2, 26,) do not account for the limitation of the reaction rate by the availability of nitrogen. They are zero order with respect to nitrogen. Mechanistically, a nitrogen-limiting function needs to be added to those formulae to represent the limitation of decreasing nitrogen concentration on decomposition rate (downregulation), for example,

$$330 \quad \frac{\partial [CN_u]}{\partial t} = -k_d f_T f_w ([CN_u] - [CN_u]_r) f([N]). \quad (30)$$

A widely used downregulation function is the Monod substrate limitation function (??):

$$f([N]) = \frac{[N]}{[N] + k_m}, \quad (31)$$

with half saturation  $k_m$ . In the case of  $[N] = k_m$ ,  $f([N]) = 0.5$ . For  $[N] \gg k_m$ , Eq. (31) is zero order with respect to  $[N]$  or has little impact on the decomposition reactions that immobilize N. For  
 335  $[N] \ll k_m$ , Eq. (31) approximates first order with respect to  $[N]$  (Figure 3d). Nevertheless, since

$$\frac{df([N])}{d[N]} = \frac{k_N}{([N] + k_m)^2}, \quad (32)$$

the derivative increases to about  $k_m^{-1}$  as the concentration decreases to below  $k_m$  (Fig. 3). This is similar to the smoothed cutoff in Eq. (28) (Fig. 2): even though it is smoothed, it is a steep transition.

To represent the threshold concentration beyond which certain microorganisms can not use certain  
340 electron donors (?), a residual concentration was added to Eq. (31):

$$f([N]) = \frac{[N] - [N]_r}{[N] - [N]_r + k_m}. \quad (33)$$

Similar to Eq. (26), this implies a nonphysical backward reaction when  $[N] < [N]_r$ . If we use the cutoff instead of a residual concentration, a combination of Eqs. (31) and (28) produces more non-linearity, as evidenced in Fig. (4), which is likely to result in small time step sizes to march through  
345 these highly nonlinear regions when the concentration gets there.

The plant nitrogen uptake reactions (R13, R14) are of zero order, and substrate limiting functions need to be added as well. For both plant uptake and immobilization, we also have to distribute the demands between  $\text{NH}_4^+$  and  $\text{NO}_3^-$ . If we simulate the  $\text{NH}_4^+$  limitation on plant uptake or immobilization with

$$350 \quad R_a = R_p \frac{[\text{NH}_4^+]}{[\text{NH}_4^+] + k_m}, \quad (34)$$

the  $\text{NO}_3^-$  plant uptake or immobilization can be represented by

$$R_n = (R_p - R_a) \frac{[\text{NO}_3^-]}{[\text{NO}_3^-] + k_m} = R_p \frac{k_m}{[\text{NH}_4^+] + k_m} \frac{[\text{NO}_3^-]}{[\text{NO}_3^-] + k_m}. \quad (35)$$

This essentially assumes an inhibition of  $\text{NH}_4^+$  on  $\text{NO}_3^-$  uptake or immobilization, and  $k_m$  becomes an inhibition coefficient. This simulates the observation that plant  $\text{NO}_3^-$  uptake rate remained  
355 low until  $\text{NH}_4^+$  concentrations dropped below a threshold (?).

For comparison with CLM, we examine the uptake rate as a function of demands and available concentrations:

$$f_{pi} = \frac{R_a + R_n}{R_p} = \frac{[\text{NH}_4^+]}{[\text{NH}_4^+] + k_m} + \left(1 - \frac{[\text{NH}_4^+]}{[\text{NH}_4^+] + k_m}\right) \frac{[\text{NO}_3^-]}{[\text{NO}_3^-] + k_m}. \quad (36)$$

As an example, we consider uptake  $R_p = 10^{-9} \text{ M s}^{-1}$  from a solution with various  $[\text{NH}_4^+]$  and  
360  $[\text{NO}_3^-]$  for a 0.5 h time step. With CLM,  $f_{pi} = 1$  when  $[\text{NH}_4^+] + [\text{NO}_3^-] \geq R_p \Delta t$ ; otherwise, it decreases with decreasing  $[\text{NH}_4^+] + [\text{NO}_3^-]$  (Fig. 5). The new representation (Eqs. 34, 35) is generally similar, with  $f_{pi} = 1$  or 0 when  $[\text{NH}_4^+]$  or  $[\text{NO}_3^-] \gg$  or  $\ll k_m$ . For the intermediate concentrations,  $f_{pi}$  in the new scheme is less than or equal to that in CLM because  $\text{NH}_4^+$  “inhibits”  $\text{NO}_3^-$  uptake. The difference decreases with decreasing  $k_m$ , disappearing at  $k_m = 10^{-10}$  (Fig. 6).

365 Various level of preferences of  $\text{NH}_4^+$  over  $\text{NO}_3^-$  were observed (?????). The microbial uptake of inorganic and organic nitrogen species is similar (?????). CLM implies a strong preference for  $\text{NH}_4^+$  over  $\text{NO}_3^-$ . For example, if  $\text{NH}_4^+$  is abundant,  $\text{NO}_3^-$  will not be taken. The new scheme allows the level of preference to be adjusted by varying  $k_m$ .

The nitrification reaction (R11) associated with decomposition to produce  $\text{N}_2\text{O}$  with the rate (Eq.  
370 4) appears as zero order as well and needs to be further downregulated as

$$\frac{\partial [\text{NH}_4^+]}{\partial t} = -2 \frac{\partial [\text{N}_2\text{O}]}{\partial t} = -f_{nm} f_T f_w f_{pH} \max(R_{nm} \frac{[\text{NH}_4^+]}{[\text{NH}_4^+] + k_m}, 0). \quad (37)$$

DC involves adding residual concentration and half saturations, which has the potential to provide mechanistic treatment of the processes. It also introduces a number of parameters that need to be determined. These parameters may not be well defined and can vary among different microbe and plant  
375 species under various conditions across the globe. An alternative is to downregulate consumption as a function of rate (DR) like CLM demand-based competition.

### 3.3.2 Downregulation of consumption as a function of rate

As described in Section 2.1.5, CLM splits the available nitrogen to meet the demands by microbes (immobilization) and plants in proportion to the potential rates (?). Suppose that the demand (consumption, sink, including immobilization, plant uptake, nitrification, etc.) rate is  $R_{dp}$ ; the supply (source, production, including deposition, mineralization, etc.) is rate  $R_s$ , and the concentration is [N] at the beginning of the time step, the demand is downregulated to  
380

$$R_d = \min \left[ R_{dp}, R_s + \frac{[N]}{\Delta t} \right]. \quad (38)$$

CLM4.5 ignores the supply term  $R_s$  (?). Applying to  $dc/dt = -1$ ,  $c^{k+1} = c^k - \Delta t$  for  $c^k \geq \Delta t$ ; for  $c^k < \Delta t$ ,  $c^{k+1} = c^k/2$ : the concentration decreases by half in a time step. This is the similar to SU with  $\alpha = 0.5$ , which is suggested by ?. DR essentially downregulates the demands using the first-order rate when nitrogen is limiting. Eq. (38) is similar to Eq. (31), except that Eq. (31) switches from zero to the first-order rate smoothly, while Eq. (38) has a discontinuity.

Implementation of DR in a geochemical code like PFLOTRAN involves separating the supply  
390 and consumption rates for each species in each reaction, and checking and conducting downregulation when necessary after contributions from all of the reactions are accumulated. It involves not only the rate terms for the residual but also the derivative terms for the Jacobian. The complexity explodes when more species needs to be downregulated (e.g.,  $\text{NH}_4^+$ ,  $\text{NO}_3^-$ , and organic N) and there are transformation processes among these species. This is shown in Appendix A, which de-  
395 scribes the implementation of downregulation of  $\text{NH}_4^+$  and  $\text{NO}_3^-$  with a nitrification reaction from  $\text{NH}_4^+$  to  $\text{NO}_3^-$ . Basically, it becomes challenging to separate, track, and downregulate consumption and production rates for an indefinite number of species, and calculation of the Jacobian becomes convoluted.

## 4 Test problems, results, and discussions

We can use SU or LT with either DC or DR, or a combination of both, to enforce nonnegativity. SU  
400 has the potential to introduce numerical error due to false convergence when STOL is satisfied and the scaling factor  $\lambda$  is too small. Stopping the simulation when  $\lambda$  is smaller than  $\lambda_{\min}$  changes the accuracy issue into a stability or robustness issue. For both SU and LT, allowing for tiny time step

sizes and an excessive number of time step cuts may transfer a stability issue into an efficiency issue.  
405 We examine the causes of negative concentration; the advantages and disadvantages of SU, LT, DC, and DR; and the accuracy, stability, and efficiency issue using both simple test problems and coupled CLM-PFLOTRAN site simulations. For simple test problems, we assess the conditions under which large updates occur. With coupled CLM-PFLOTRAN spin-up simulations for arctic, temperate, and tropical sites, we assess the conditions when the nonnegativity issue arises by relaxing the  
410 downregulation on nitrogen consumption (decreasing half saturation). Spreadsheet, python scripts, and PFLOTRAN input files for these simple test problems and for producing figures are provided as supplemental information.

Our implementation of CLM biogeochemistry introduces mainly two parameters: half saturation  $k_m$  and residual concentration. A wide range of  $k_m$  values were reported for  $\text{NH}_4^+$ ,  $\text{NO}_3^-$ , and organic  
415 nitrogen for microbes and plants. The median, mean, and standard deviations range from  $10 \sim 100$ ,  $50 \sim 500$ , and  $10 \sim 200 \mu\text{M}$ , respectively (?). Reported residual (threshold) concentrations are limited and are considered to be 0 (e.g., ?), likely because of the detection limits of the analytical methods. The detection limits are usually at the  $\mu\text{M}$  level, while up to the  $\text{nM}$  level was reported  
420 (?). In Ecosys, the  $k_m$  is 0.40 and  $0.35 \text{ gN m}^{-3}$ , and the residual concentration is 0.0125 and  $0.03 \text{ gN m}^{-3}$  (?) for  $\text{NH}_4^+$  and  $\text{NO}_3^-$  for microbes. Depending on the moisture content, say 10, 100, and 1000  $\text{L m}^{-3}$  for a dry, wet, and saturated case, these  $k_m$  values roughly translate to  $10^{-3}$ ,  $10^{-4}$ , and  
425  $10^{-5} \text{ M}$ . We start with  $k_m = 10^{-6} \text{ M or mol m}^{-3}$ , and residual concentration  $10^{-15} \text{ M or mol m}^{-3}$  for plants and microbes. To further investigate the nonnegativity challenge for the current study and for future application for other nutrients (e.g.,  $\text{H}_2$  and  $\text{O}_2$ ) where the concentrations can be much  
430 lower, we examine  $k_m$  from  $10^{-3}$  to  $10^{-12}$  in our test problems. The  $k_m$  is expected to be different for different plants, microbes, and for  $\text{NH}_4^+$  and  $\text{NO}_3^-$ , and different values can be assigned in the input file in our implementation. we do not differentiate them in this work as we focus on numerical issues.

#### 4.1 Plant nitrogen uptake, nitrification, and denitrification

430 It was observed that plants can decrease nitrogen concentration to below detection limits in hours (?). Plant nitrogen uptake is one of the major sinks for nitrogen in TEMs and contributes to decreasing nitrogen concentration numerically to 0 or negative. In CLM, the total plant nitrogen demand is calculated based on photosynthesized carbon allocated for new growth and the C:N stoichiometry for new growth allocation, and the plant nitrogen demand from the soil is equal to the total  
435 nitrogen demand minus retranslocated nitrogen stored in the plants (?). The CLM calculated rate is provided as an input to PFLOTRAN, which is constant in a 0.5 h time step. Without downregulating plant nitrogen uptake rate, nitrogen concentration is likely to go negative when the net consumption rate overwhelms a low available concentration. As the Monod substrate limiting function is the most widely used downregulation function, we examine the numerical solutions, beginning with the

440 numerical issues during the iteration processes. Incrementally, we add first order reactions (e.g., nitrification, denitrification, and plant  $\text{NO}_3^-$  uptake) to look into these issues in increasingly complex systems.

#### 4.1.1 Plant $\text{NH}_4^+$ uptake (Test 1)

We consider the plant  $\text{NH}_4^+$  uptake reaction (R13) with the rate  $R_a$  downregulated by the Monod  
445 substrate limiting function:

$$\frac{d[\text{NH}_4^+]}{dt} = -R_a \frac{[\text{NH}_4^+]}{[\text{NH}_4^+] + k_m} = -R_{at}. \quad (39)$$

As an analytical solution is not available, discretizing Eq. (39) using the backward difference, it becomes

$$[\text{NH}_4^+]^{k+1} + (k_m + R_a \Delta t - [\text{NH}_4^+]^k) [\text{NH}_4^+]^{k+1} - k_m [\text{NH}_4^+]^k = 0. \quad (40)$$

450 The two roots are

$$[\text{NH}_4^+]^{k+1} = 0.5 \left[ [\text{NH}_4^+]^k - k_m - R_a \Delta t \pm \sqrt{([\text{NH}_4^+]^k - k_m - R_a \Delta t)^2 + 4k_m [\text{NH}_4^+]^k} \right]. \quad (41)$$

One root is positive, and the other is negative (not physical). With the positive root,  $[\text{NH}_4^+]^{k+1} \rightarrow 0$  when  $[\text{NH}_4^+]^k \rightarrow 0$ , or  $R_a \Delta t \rightarrow \infty$ . As  $k_m \rightarrow 0$ ,  $[\text{NH}_4^+]^{k+1} \rightarrow 0$  when  $[\text{NH}_4^+]^k \leq R_a \Delta t$ . If we replace  $[\text{NH}_4^+]$  with  $[\text{NH}_4^+] - [\text{NH}_4^+]_r$  in Eqs. (39) and (41),  $[\text{NH}_4^+]^{k+1} \rightarrow [\text{NH}_4^+]_r$  rather than 0. We  
455 do not include the residual concentration in the simple test problems for simplicity in this subsection.

Ignoring the negative root, the representation of plant  $\text{NH}_4^+$  uptake by Eq. (39) ensures  $[\text{NH}_4^+]^{k+1} \geq [\text{NH}_4^+]_r$  or 0.

Solving Eq. (39) using the Newton-Rapshon method from time step  $k$  to  $k+1$ , the update is

$$\delta[\text{NH}_4^+]^{k+1,p} = \frac{\frac{[\text{NH}_4^+]^{k+1,p} - [\text{NH}_4^+]_k}{\Delta t} + R_a \frac{[\text{NH}_4^+]^{k+1,p}}{[\text{NH}_4^+]^{k+1,p} + k_m}}{\frac{1}{\Delta t} + R_a \frac{k_m}{([\text{NH}_4^+]^{k+1,p} + k_m)^2}}. \quad (42)$$

460 For the first iteration,  $[\text{NH}_4^+]^{k+1,0} = [\text{NH}_4^+]^k$ ,

$$\xi = \frac{\delta[\text{NH}_4^+]^{k+1,1}}{[\text{NH}_4^+]^{k+1,0}} = \frac{\frac{1}{[\text{NH}_4^+]^k + k_m}}{\frac{1}{R_a \Delta t} + \frac{k_m}{([\text{NH}_4^+]^k + k_m)^2}}. \quad (43)$$

The update is a function of uptake rate ( $R_a$ ), time step size ( $\Delta t$ ), concentration ( $[\text{NH}_4^+]^k$ ), and half saturation ( $k_m$ ).

For  $R_a\Delta t$  from 0 to  $\infty$ ,  $\xi$  increases from 0 to  $1 + [\text{NH}_4^+]/k_m$ . With  $[\text{NH}_4^+]^k = 10^{-6}$  M, and  $k_m = 10^{-6}$  M, the update is less than  $[\text{NH}_4^+]^k$  when  $R_a\Delta t \leq 5 \times 10^{-6}$  M (say using CLM  $\Delta t = 1800$  s,  $R_a \leq 2.8 \times 10^{-9}$  mol s $^{-1}$ , Fig. 7); when  $R_a\Delta t$  increases, the update increases, with an upper limit of 2, suggesting that large time step size and uptake rate alone usually do not lead to an excessively large update or a small scaling factor.

For  $[\text{NH}_4^+]^k$  from 0 to  $\infty$ ,  $\xi$  starts from  $R_a\Delta t/(k_m + R_a\Delta t)$ , increases to peak at  $\sqrt{R_a\Delta t/k_m}/2$  when  $[\text{NH}_4^+] = \sqrt{k_m R_a \Delta t} - k_m$ , and then decreases to 0. With  $k_m = 10^{-6}$  M and  $R_a\Delta t = 0.001$  M,  $\xi$  starts from  $\sim 1$ , increases to peak at  $\sim 16$  when  $[\text{NH}_4^+]^k = 3 \times 10^{-5}$ , and decreases to 0 as  $[\text{NH}_4^+]^k \rightarrow \infty$ .

For  $k_m$  from  $\infty$  to 0,  $\xi$  increases from 0 to  $R_a\Delta t/k_m$ . With  $R_a\Delta t = 10^{-3}$ , and  $[\text{NH}_4^+]^k = 10^{-6}$ , the update increases several orders of magnitude as  $k_m$  decreases from  $10^{-6}$  to  $10^{-9}$ , with a limit of  $\xi = 10^3$  (Fig. 7).

While the semi-analytical solution (Eq. 41) indicates that the problem itself is nonnegative, these calculations suggests that overshoot can occur, and large time step, uptake rate, low concentration and half saturation can contribute to large update that can exceed the available concentration by orders of magnitude.

Now we look into the iteration processes: the solution starts with an overshoot to  $1.995 \times 10^{-6}$  and converges to the positive semi-analytical solution  $3.1127 \times 10^{-5}$  (Eq. 41) in eight iterations when  $R_a\Delta t = 0.001$  (Table 1). dR/dC changes from  $\sim 1$  to  $10^5$  in the first iteration, although the change in the Jacobian is reduced due to a small  $R_a\Delta t$ . With  $R_a\Delta t = 0.002$ , the update  $\delta$  is greater than  $[\text{NH}_4^+]_k$ ; without scaling back the update, the solution converges to the negative solution  $-1.002 \times 10^{-3}$  (Table 2, negative root from Eq. 41). Scaling back the update with  $\alpha = 0.9999$ , the concentration decreases by  $1 - \alpha = 10^{-4}$  times in the first iteration rather than to negative root (Table 3). The solution converges to the positive root in seven iterations.

If LT is used with  $R_a\Delta t = 0.002$ , the solution oscillates and results in a  $\delta$  of  $-1041.5$  in the fifth iteration, which essentially makes the solution 0 (Table 4). Limiting  $\delta \leq \delta_{\ln,\max}$ , the solution converges to the semi-analytical solution (Eq. 41) in 7, 7, 6, 5, 6, and 8 iterations with  $\delta_{\ln,\max} = 2, 3, 4, 5, 6$ , and 7, respectively. For  $\delta_{\ln,\max} \geq 8$ , the iteration oscillates and converges slowly. If we split  $R_a\Delta t = 0.002$  into two steps, the first step takes seven iterations to converge, while the second step takes nine iterations, with  $\delta_{\ln,\max} = 5$ . These simulations show that limiting the update to be less than  $\delta_{\ln,\max}$  is helpful for LT to use large time step sizes for efficiency.

Finally, we consider a PFLOTRAN simulation: a 1 m  $\times$  1 m  $\times$  1 m grid cell, with 0.25 water content, initial 4  $\mu\text{M}$   $\text{NH}_4^+$ , and a plant  $\text{NH}_4^+$  demand  $10^{-7}$  mol s $^{-1}$  ( $\sim 3$  mg d $^{-1}$ , reported values for evergreen and deciduous forest range from  $0.3 \sim 10$  g m $^{-2}$  year, ?, ?). It takes 10,000 s (2.78 h) to consume  $\text{NH}_4^+$ . We use a time step of 0.5 h for a simulation duration of 10 h. Without downregulating the uptake rate, SU decreases  $[\text{NH}_4^+]$  to 0 and then keeps it 0 as  $\lambda = 0$ . With LT, we obtain an accurate solution until it fails when the concentration goes to 0, and the Jacobian becomes singular.

Using SU with DC with  $[\text{NH}_4^+]_r$  of  $10^{-20}$  M (Eq. 33) and a half saturation  $k_m$  of  $10^{-6}$ ,  $10^{-9}$ , or  $10^{-12}$ , the calculated concentration  $[\text{NH}_4^+]$  is kept to be greater than or equal to  $10^{-20}$  (Figure. 8). With a  $k_m$  of  $10^{-6}$ , the calculated  $[\text{NH}_4^+]$  is above  $10^{-20}$ , and the update does not exceed the concentration in any iteration during the 10 h simulation duration. With a  $k_m$  of  $10^{-9}$  and  $10^{-12}$ , 505 the update exceeds the concentration from time 2.5 h to 3.0 h. In the case of  $k_m = 10^{-12}$  M for the next time step, the two iterations decrease the concentration by 10,000 times, and the solution is deemed converged as the default  $\text{STOL} = 10^{-8}$  is met. This continues for another time step with one iteration (Fig. 8). In these two time steps, the solution does not converge to the exact solution. If we set the residual concentration to  $10^{-15}$ , the false convergence results in a concentration below  $10^{-15}$  510 ( $8.71 \times 10^{-16}$ ) in the first of the two time steps. If we set  $\text{STOL} = 10^{-50}$  to avoid the convergence due to Eq. (17), PFLOTTRAN cuts the time step sizes and quits due to too many cuts.

Using LT can avoid the false convergences in this example, but it requires more iterations, with 56/95, 36/110, and 32/87 for SU/LT for  $k_m$  values of  $10^{-6}$ ,  $10^{-9}$ , and  $10^{-12}$  M, respectively. These results demonstrate that SU ensures nonnegativity and allows large time step for efficiency at the 515 risk of inaccuracy. LT is accurate but requires more iterations.

#### 4.1.2 Plant $\text{NH}_4^+$ uptake and nitrification (Test 2)

Adding a nitrification reaction (R10) with a first-order rate, Eq. (39) becomes

$$\frac{d[\text{NH}_4^+]}{dt} = -R_a \frac{[\text{NH}_4^+]}{[\text{NH}_4^+] + k_m} - k_{nitr} [\text{NH}_4^+] = -R_{at} - R_{nitr}. \quad (44)$$

Discretizing the equation in time using the backward difference,

$$520 \quad (1 + k_{nitr} \Delta t)[\text{NH}_4^+]^{k+1}^2 + (k_m + R_a \Delta T + k_{nitr} k_m \Delta t - [\text{NH}_4^+]^k) \text{NH}_4^+^{k+1} - k_m [\text{NH}_4^+]^k = 0. \quad (45)$$

Denote  $-b = k_m + R_a \Delta T + k_{nitr} k_m \Delta t - [\text{NH}_4^+]^k$ , the roots are

$$[\text{NH}_4^+]^{k+1} = \frac{\left[ b \pm \sqrt{b^2 + 4(1 + k_{nitr} \Delta t)[\text{NH}_4^+]^k k_m} \right]}{2(1 + k_{nitr} \Delta t)}. \quad (46)$$

Similar to Eq. (39), one root is nonnegative. To solve the problem with the Newton-Raphson method, the equation is

$$525 \quad \begin{bmatrix} \frac{1}{\Delta t} + J_{at} + J_{nitr} & 0 & 0 \\ -J_{at} & \frac{1}{\Delta t} & 0 \\ -J_{nitr} & 0 & \frac{1}{\Delta t} \end{bmatrix} \begin{pmatrix} \delta[\text{NH}_4^+]^{k+1,1} \\ \delta[\text{PlantA}]^{k+1,1} \\ \delta[\text{NO}_3^-]^{k+1,1} \end{pmatrix} = \begin{pmatrix} R_{at} + R_{nitr} \\ -R_{at} \\ -R_{nitr} \end{pmatrix}, \quad (47)$$

with  $J_{at} = \frac{dR_{at}}{d[\text{NH}_4^+]} = R_a \frac{k_m}{([\text{NH}_4^+] + k_m)^2}$ , and  $J_{nitr} = \frac{dR_{nitr}}{d[\text{NH}_4^+]} = k_{nitr}$ . The solutions are

$$\delta[\text{NH}_4^+]^{k+1,1} = \frac{R_{at} + R_{nitr}}{\frac{1}{\Delta t} + J_{at} + J_{nitr}}, \quad (48)$$

$$\delta[\text{PlantA}]^{k+1,1} = J_{at} \delta[\text{NH}_4^+]^{k+1,1} - R_{at} = -\frac{\frac{1}{\Delta t} + J_{nitr}}{\frac{1}{\Delta t} + J_{at} + J_{nitr}} R_{at} + \frac{J_{at}}{\frac{1}{\Delta t} + J_{at} + J_{nitr}} R_{nitr}, \quad (49)$$

and

$$530 \quad \delta[\text{NO}_3^-]^{k+1,1} = J_{nitr} \delta[\text{NH}_4^+]^{k+1,1} - R_{nitr} = \frac{J_{nitr}}{\frac{1}{\Delta t} + J_{at} + J_{nitr}} R_{at} - \frac{\frac{1}{\Delta t} + J_{at}}{\frac{1}{\Delta t} + J_{at} + J_{nitr}} R_{nitr}. \quad (50)$$

It is not a surprise for  $\delta[\text{NH}_4^+]^{k+1,1}$  to be positive as plant  $\text{NH}_4^+$  uptake and nitrification consume  $\text{NH}_4^+$ . It is a little surprising that a positive component,  $\frac{J_{at}}{1/\Delta t + J_{at} + J_{nitr}} R_{nitr}$ , is introduced to  $\delta[\text{PlantA}]^{k+1,1}$  even though there is no reaction that consumes PlantA. Depending on the relative magnitude of the rates ( $R_{at}$  and  $R_{nitr}$ ) and the derivatives ( $J_{at}$  and  $J_{nitr}$ ), as well as time step size  $\Delta t$  and  $[\text{NH}_4^+]^k$ , the update can be positive, which can result in too small a scaling factor that causes a nonnegativity issue if [PlantA] is very small. This demonstrates that products as well as reactants can be driven negative during the Newton-Raphson iterations (overshoot).

This can also be shown with another simple first-order reaction  $A \rightarrow B$  with rate  $k[A]$ : taking out the equation for B,  $-k\delta[A] + \delta[B]/\Delta t = -k[A]$ ,  $\delta[B] = k\Delta t(\delta[A] - [A])$ . Suppose  $\delta[A] = 2 \times 10^{-6}$ ,  $[A] = 10^{-6}$ , and  $k\Delta t = 10^{-3}$ , then  $\delta[B] = 10^{-9}$ . If  $[B]$  is very small, say  $10^{-20}$ , this results in a  $\lambda = 0.99 \times 10^{-11}$ . This has an implication for DR: downregulating only some reactants may not be sufficient to guarantee positivity, while downregulating all species is complicated.

The update  $\delta\text{NO}_3^-$  can be positive, and cause negative consequence for the calculation as well. It can become worse when the same Monod substrate limiting function is used to further downregulate the nitrification rate like CLM demand based competition, namely,  $R_{nitr} = k_{nitr}[\text{NH}_4^+] \frac{[\text{NH}_4^+]}{[\text{NH}_4^+] + k_m}$ ,  $J_{nitr} = k_{nitr} \frac{[\text{NH}_4^+]}{[\text{NH}_4^+] + k_m} + k_{nitr}[\text{NH}_4^+] \frac{k_m}{([\text{NH}_4^+] + k_m)^2} = k_{nitr} \frac{[\text{NH}_4^+]}{[\text{NH}_4^+] + k_m} \left(1 + \frac{k_m}{[\text{NH}_4^+] + k_m}\right)$ . For  $[\text{NH}_4^+] \ll k_m$ , this increases  $J_{nitr}$  approximately by the order of  $k_m^{-1}$ , which can result in an increase of the update.

### 4.1.3 Plant uptake, nitrification, and denitrification (Test 3)

550 Adding plant  $\text{NO}_3^-$  uptake reaction (R14) with rate  $R_{nt} = R_p \frac{[\text{NH}_4^+]}{[\text{NH}_4^+] + k_m} \frac{[\text{NO}_3^-]}{[\text{NO}_3^-] + k_m}$ ,  $J_{nt,n} = \frac{dR_{nt}}{d[\text{NO}_3^-]} = R_p \frac{[\text{NH}_4^+]}{[\text{NH}_4^+] + k_m} \frac{k_m}{([\text{NO}_3^-] + k_m)^2}$ , and  $J_{nt,a} = \frac{dR_{nt}}{d[\text{NH}_4^+]} = \frac{dR_n}{d[\text{NH}_4^+]} \frac{k_m}{([\text{NH}_4^+] + k_m)^2} \frac{[\text{NO}_3^-]}{[\text{NO}_3^-] + k_m}$ , and denitrification reaction (R12) with rate  $R_{deni} = k_{deni} [\text{NO}_3^-]$ , and  $J_{deni} = \frac{dR_{deni}}{d[\text{NO}_3^-]} = k_{deni}$ , the equation becomes

$$\begin{bmatrix} \frac{1}{\Delta t} + J_{at} + J_{nitr} & 0 & 0 & 0 & 0 \\ -J_{at} & \frac{1}{\Delta t} & 0 & 0 & 0 \\ -J_{nitr} + J_{nt,a} & 0 & \frac{1}{\Delta t} + J_{nt} + J_{deni} & 0 & 0 \\ -J_{nt,a} & 0 & -J_{nt,n} & 1/\Delta t & 0 \\ 0 & 0 & -0.5J_{deni} & 0 & 1/\Delta t \end{bmatrix} \begin{pmatrix} \delta[\text{NH}_4^+]^{k+1,1} \\ \delta[\text{PlantA}]^{k+1,1} \\ \delta[\text{NO}_3^-]^{k+1,1} \\ \delta[\text{PlantN}]^{k+1,1} \\ \delta[\text{N}_2]^{k+1,1} \end{pmatrix} = \begin{pmatrix} R_{at} + R_{nitr} \\ -R_{at} \\ -R_{nitr} + R_{nt} + R_{deni} \\ -R_{nt} \\ -0.5R_{deni} \end{pmatrix}. \quad (51)$$

As a result,

$$\delta[\text{NO}_3^-]^{k+1,1} \left( \frac{1}{\Delta t} + J_{nt} + J_{deni} \right) = (J_{nitr} - J_{nt,a}) (R_{at} + R_{nitr}) \delta[\text{NH}_4^+]^{k+1,1} - R_{nitr} + R_{nt} + R_{deni}, \quad (52)$$

555

and

$$\delta[\text{PlantN}]^{k+1,1} / \Delta t = J_{nt,a} \delta[\text{NH}_4^+]^{k+1,1} + J_{nt,n} \delta[\text{NO}_3^-]^{k+1,1} - R_{nt}. \quad (53)$$

In addition to plant  $\text{NH}_4^+$  uptake and nitrification,  $\delta[\text{NO}_3^-]^{k+1,1}$  becomes a function of plant  $\text{NO}_3^-$  uptake and denitrification, and all of the rate coefficients and derivatives may contribute to a positive update that can result in too small a scaling factor. Even though the problem itself is nonnegative, coupling these reactions together in the Newton-Raphson iteration does introduce the potential to produce relatively significant positive update for  $\text{NO}_3^-$  and PlantN. It worsens when the preference-based uptake of  $\text{NH}_4^+$  over  $\text{NO}_3^-$  (Eqs. 34 and 35) brings in the impact of any rates related to  $\text{NH}_4^+$  (including deposition, uptake, immobilization, etc.), with potentially large derivative terms for the off-diagonal entries in the Jacobian matrix. It is the nonlinearity introduced in the downregulation and propagated through the reactions that causes the challenge. A smaller half saturation introduces a greater derivative change; therefore, it is more likely to cause the problem. These results also suggest that the likelihood for  $\text{NO}_3^-$  to go negative is greater than  $\text{NH}_4^+$ , and PlantN is greater than PlantA as the latter are influenced by more rates and derivatives.

### 570 4.2 N immobilization, mineralization, and nitrification during decomposition (Test 4)

We further examine the implications of a small half saturation on the numerical solutions with a decomposition test problem. We consider a case of decomposing 0.2 M Lit1C + 0.005 M Lit1N to

produce SOM1 with an initial  $4 \mu\text{M}$   $\text{NH}_4^+$  using the reactions (R7 and R2) in the CLM-CN reaction network (Fig. 1) at first. Then we add the nitrification reaction (R11) with rate (Eq. 37) to examine  
575 the implications of a complex rate formula. We use PFLOTRAN with a fully saturated grid cell of 1 m and porosity of 0.25.

Lit1 decomposes fast at the beginning and then slows down as  $\text{NH}_4^+$  is depleted (Fig. 9). The Lit1 decomposition rate is controlled by the mineralization rate from SOM1 decomposition. As the immobilization rate decreases with decreasing Lit1,  $[\text{NH}_4^+]$  rebounds. For  $k_m$  of  $10^{-6}$ ,  $10^{-9}$ ,  
580 and  $10^{-12} \text{ M}$ , Lit1 and SOM1 dynamics are similar, but the  $[\text{NH}_4^+]$  values are decreased to  $\sim 10^{-8}$ ,  $10^{-11}$ , and  $10^{-14} \text{ M}$ , respectively. The number of iterations for SU/LT is 76/169, 68/194, and 54/207 for the three  $k_m$  values. Obviously, smaller  $k_m$  results in lower  $[\text{NH}_4^+]$  and more iterations.

The implication of  $k_m = 10^{-12}$  becomes obvious when the nitrification reaction (R11) with rate (Eq. 37) is included. In the time step when the mineralization rate surpasses the immobilization,  
585  $\delta[\text{N}_2\text{O}] > [\text{N}_2\text{O}]$ , and  $\text{N}_2\text{O}$  is lowered to  $10^{-23} \text{ M}$  in three iterations as STOL is met. In the next time step,  $\delta[\text{N}_2\text{O}] = \sim 10^{-13}$ , resulting in a scaling factor  $\lambda$  of  $10^{-10}$  that stops the simulation. Checking the calculations in the last iteration, the lower  $\text{NH}_4^+$  concentration ( $2 \times 10^{-13} \text{ M}$ ) introduces a derivative ( $6.94 \times 10^{11}$ ) into the column of the Jacobian with respect to  $\text{NH}_4^+$ . Because  $\text{N}_2\text{O}$  production is a function of both immobilization and mineralization, a Monod substrate limiting function  
590 is added to downregulate the mineralization component (Eq. 37). In the row corresponding to  $\text{N}_2\text{O}$ , the off-diagonal terms are nonzero in the entries with respect to  $\text{NH}_4^+$ , Lit1C, Lit1N, and SOM1. Even though these values are relatively small because the fraction of net mineralization rate to  $\text{N}_2\text{O}$  is small (0.02), inversion of the Jacobian matrix results in substantial values in the row, and the  $10^{-13} \text{ M}$  update comes mainly from the entries with respect to Lit1C and Lit1N. This further  
595 illustrates that extremely small half saturation together with complex rate limiting formula can result in large derivatives at small concentration, which may lead to overshoot that results in a small update scaling factor.

### 4.3 CLM-PFLOTRAN simulations

We examine the nonnegative challenge in the coupled CLM-PFLOTRAN simulations for arctic  
600 (US-Brw), temperate (US-WBW), and tropical (BR-Cax) AmeriFlux sites. The CLM-PFLOTRAN simulations are run in the mode that PFLOTRAN only handles subsurface chemistry (decomposition, nitrification, denitrification, N plant uptake). For comparison, 1) depth and  $\text{O}_2$  availability impact on decomposition, 2) cryoturbation, and 3) SOM transport are ignored by setting 1) decomp\_depth\_efolding to  $10^6 \text{ m}$ , o\_scalar to 1, 2) cryoturb\_diffusion and 3) som\_diffusion to 0. For  
605 CLM-PFLOTRAN simulations,  $k_m = 10^{-6}$  and residual concentration  $10^{-15}$  are used for the base case. The nonnegativity challenge is assessed in particular by relaxing the downregulation (decreasing  $k_m$ ). Nitrogen is the focus as it is the rate limiting nutrient in CLM4.5 biogeochemistry. Spin-up simulations are used because they are generally more likely to face a nonnegativity challenge be-

cause the simulations start far away from equilibrium. In these site simulations, PFLOTRAN uses  
610 the same 10 layer grid for the 3.8 m one-dimensional column as CLM. The simulation duration is  
500, 300, and 300 year for the arctic, temperate, and tropical sites as the system roughly reaches  
steady state within these simulation durations.

### 4.3.1 Site descriptions

The US-Brw site (71.35N,156.62W) is located near Barrow, Alaska. The mean annual temperature,  
615 precipitation, and snowfall are  $-12^{\circ}\text{C}$ , 11 cm, and 69 cm, respectively (1971  $\sim$  2000) (?). The  
landscape is poorly drained polygonized tundra. The maximum thaw depth ranges from 30 to 40 cm,  
and the snow free-period is variable in length but generally begins in early June and lasts until early  
September (?). The area is composed of several different representative wet-moist coastal sedge  
tundra types, including wet sedges, grasses, moss, and assorted lichens. The leaf area index (LAI) is  
620  $\sim 1.1$ .

The US-WBW site (35.96N, 84.29W) is located in the Walker Branch Watershed in Oak Ridge,  
Tennessee (?). The climate is typical of the humid southern Appalachian region. The mean annual  
precipitation is  $\sim 139$  cm, and the mean median temperature is  $14.5^{\circ}\text{C}$ . The soil is primarily Ultisols  
that developed in humid climates in the temperate zone on old or highly weathered material under  
625 forest. The temperate deciduous broadleaf forest was regenerated from agriculture land 50 years  
ago. LAI is  $\sim 6.2$  (?).

The BR-Cax site (-1.72N, -51.46W) is located in the eastern Amazon tropical rainforest. The  
mean annual rainfall is between 2000 and 2500 mm, with a pronounced dry season between June  
and November. The soil is a yellow oxisol (Brazilian classification latossolo amarelo) with a thick  
630 stony laterite layer at 3  $\sim$  4 m depth (?). The vegetation is evergreen broadleaf forest. The LAI is 4  
 $\sim 6$  (?).

### 4.3.2 Base case simulation results

For CLM-PFLOTRAN base case simulations, we use DC and LT because DC is the general geo-  
chemical modeling approach and is rigorous, and LT is less likely to cause numerical error than SU.  
635 The site climate data from 1998 to 2006, 2002 to 2010, and 2001 to 2006 are used to drive the spin-up  
simulation for the arctic, temperate, and tropical sites, respectively. This introduces a multi-year cy-  
cle in addition to the annual cycle (Figs. 10, 11, 12). Overall, CLM-PFLOTRAN roughly reproduces  
CLM4.5 in predicting LAI and nitrogen distribution among vegetation, litter, SOM,  $\text{NH}_4^+$  and  $\text{NO}_3^-$   
640 pools for the arctic (Fig. 10), temperate (Fig. 11), and tropical site (Fig. 12). CLM calculation does  
accumulate more SOMN (nitrogen in the four SOM pools) than CLM-PFLOTRAN as the simulation  
is close to equilibrium, resulting in higher  $[\text{NH}_4^+]$  and  $[\text{NO}_3^-]$  in CLM than CLM-PFLOTRAN at  
later times. This will be further investigated in future work while the current work focuses on non-

negativity. Despite these differences, the calculated LAI, VEGN (vegetation N), and LITN (nitrogen in the three litter pools) are very close.

645 The arctic site shows a distinct summer growing season (Fig. 10): LAI and VEGN jump up at the beginning, then level off, and drop down at the end of the growing season when LITN jumps up due to litter fall.  $\text{NH}_4^+$  and  $\text{NO}_3^-$  drop to very low level at the beginning of growing season and accumulate at the other times. In addition to a longer growing season than the arctic site, the temperate site shows more litter fall by the end of the growing season as it is a temperate deciduous  
650 forest, which introduces immobilization demand that further lowers  $\text{NH}_4^+$  and  $\text{NO}_3^-$  concentrations (Fig. 11e inset). The seasonality is much less apparent in the tropical site than in the arctic and temperate sites. LAI, VEGN, LITN, and SOMN accumulate with less seasonal variations to reach an equilibrium. It takes much longer simulation duration to spin up the simulation for the arctic site than the temperate and tropical sites because the latter receive more solar radiation.

655 Except for the tropical site where the higher  $k_m$  of  $10^{-3}$  mol m $^{-3}$  results in lower immobilization, higher accumulation of LITN, and higher  $[\text{NH}_4^+]$  and  $[\text{NO}_3^-]$  during the spinup (Fig. 12), the range of  $k_m$  values ( $10^{-3}$ ,  $10^{-6}$ , and  $10^{-9}$  mol m $^{-3}$ ) generally has limited impact on the overall calculations except that the nitrogen concentrations drop lower with lower  $k_m$  values (e.g., inset in Figs. 10e,f, 11e), which is similar to Fig. (9). The lack of sensitivity is because these very low concentrations  
660 do not make up a mass of nitrogen that is significant enough to influence the carbon and nitrogen cycle. However, as a small  $k_m$  value means weak downregulation and steep transition between zero order and first order, it has implications on the accuracy, stability, and efficiency of the numerical solutions.

### 4.3.3 Efficiency

665 We use OIC (ORNL Institutional Cluster phase5 esd13q) for the comparison of computing time for the three sites using DC or DR with SU or LT. The results suggest that SU takes about 30~80% more time than CLM, and LT costs about two to four times that of CLM (Table 5). For LT with DC, the computing time increases with decreasing  $k_m$ . This is expected because a smaller  $k_m$  may require smaller time step size to march through steeper transition. The computing time appears not  
670 to be infeasibly high. The comparison between DC and DR is mixed. This is because DC has more complicated substrate limiting representation that requires smaller time step sizes to march through steep transitions, while DR has simpler substrate limiting representation, but a discontinuity that may require more iterations. We expect that CLM-PFLOTRAN will require more computational cost as more complex biogeochemical processes are represented, transport is added, and thermal  
675 hydrology (including freeze and thaw) are incorporated. Future code optimization for performance on next-generation supercomputers is expected to mitigate the computational cost.

#### 4.3.4 Accuracy

We use the tropical site to demonstrate the accuracy issue by SU (scaling update); i.e., the small scaling factor ( $\lambda$ ) may not only limit N consumption (immobilization and uptake) to account for availability limitation but also “inhibit” accumulation from mineralization, deposition, and fixation.

With  $k_m = 10^{-3}$  mol m<sup>-3</sup>, the LAI, VEGN, LITN, SOMN, NH<sub>4</sub><sup>+</sup>, and NO<sub>3</sub><sup>-</sup> are similar to that calculated using LT (Fig. 12 vs. 13). With decreasing  $k_m$ , the results diverge by SU but not by LT. With  $k_m$  of 10<sup>-6</sup> mol m<sup>-3</sup>, much less nitrogen is predicted to accumulate with SU than with LT.

Checking NH<sub>4</sub><sup>+</sup> and NO<sub>3</sub><sup>-</sup> concentration in the first year, SU calculation is similar to LT when NH<sub>4</sub><sup>+</sup> and NO<sub>3</sub><sup>-</sup> are abundant due to nitrogen mineralization from SOM4 decomposition at early times (Fig. 14). As nitrogen becomes limiting at late times due to increased plant nitrogen demand, NH<sub>4</sub><sup>+</sup> and NO<sub>3</sub><sup>-</sup> accumulate lower by SU than by LT. Further checking into the daily cycles (Fig. 14 inset) reveals that NH<sub>4</sub><sup>+</sup> and NO<sub>3</sub><sup>-</sup> accumulate during the night when photosynthesis and plant nitrogen uptake pause. As the sun rises, photosynthesis and plant nitrogen uptake resume, decreasing nitrogen concentrations to very low level, limiting further uptake. As a result, nitrogen rebounds and then decreases again until sunset. From day 226 to 230, SU calculations are only slightly lower than LT calculations during the rebound. From day 250 to 254, the SU calculated rebounds are much lower than LT calculations. From day 295 to 300, accumulation during both night and day are decreased. Overall, NH<sub>4</sub><sup>+</sup> and NO<sub>3</sub><sup>-</sup> accumulation appear to be numerically “inhibited” when the system becomes increasingly nitrogen limiting and when SU is used.

Finally checking nitrogen dynamics between day 250 and 254, these “inhibited” intervals in Fig. (14) coincide with the concentration valleys in the diagnostic species N<sub>2</sub>Od, which is used to track N<sub>2</sub>O production (reaction R11) due to decomposition (Eq. 37, Fig. 15). At the beginning of each CLM 0.5 h time step, we reset [N<sub>2</sub>Od] to 10<sup>-10</sup> in PFLTRAN so that it can be used to calculate the reaction rate for CLM (instead of saving concentration in previous time step) As we do not have any consumption reaction for N<sub>2</sub>Od, the decreases are purely numerical. The contribution of the derivatives of the rate (Eq. 37) results in a large enough positive update to N<sub>2</sub>Od, which results in a small scaling factor, and the solution is considered converged due to less than STOL update. This small scaling factor and false convergence result in the “inhibition” of NH<sub>4</sub><sup>+</sup> and NO<sub>3</sub><sup>-</sup> production, and manifest as much less nitrogen accumulation in Fig. (13). If we remove the contribution of the derivatives for Eq. (37) for the entries with respect to N<sub>2</sub>Od from the Jacobian, the “inhibition” disappears and SU results become close to LT (Fig. 15). If we decrease STOL from 10<sup>-8</sup> to 10<sup>-50</sup>, and  $\lambda_{min}$  from 10<sup>-10</sup> to 10<sup>-50</sup>, the false convergence occurs less often and the difference from LT decreases. This can also be mitigated by increasing the value from 10<sup>-10</sup> to 10<sup>-6</sup> that we reset these diagnostic species concentrations.

An alternative to mitigate the issue is to use DR rather than DC. The rate formulae for DR can be very simple (no need for substrate limiting function). Because we use  $k_m$  to distribute nitrogen  
715 demand between  $\text{NH}_4^+$  and  $\text{NO}_3^-$  (Eqs. 34 and 35) for plant nitrogen uptake and immobilization, our implementation ends up with the difference between DC and DR as that DR does not have  $\text{NO}_3^-$  substrate limiting terms and uses Eq. (38) for downregulation of both  $\text{NH}_4^+$  and  $\text{NO}_3^-$ . With DR, the numerical error is much reduced (Fig. 13 vs. 16). However, it increases slightly with decreasing  $k_m$  when comparing with LT (not shown). These results show that decreasing the complexity of the rate  
720 limiting representation helps reducing the nonnegativity challenge for SU.

#### 4.3.5 Stability and robustness

PFLOTTRAN may stop CLM-PFLOTTRAN run due to 1) too small a scaling factor for SU to avoid excessive numerical error, 2) too small a time step size or too many time step cuts for either SU or LT, and 3) singular Jacobian matrix for LT.

725 With SU and DC, the simulations run to conclusion for  $k_m = 10^{-3}$ ,  $10^{-6}$ , and  $10^{-9} \text{ mol m}^{-3}$  but abort for  $k_m = 10^{-12}$  for all of the three sites (Table 6). The reasons for the unfinished runs are too small a scaling factor for  $\text{NO}_3^-$  (Table 6). As indicated in Test 3, it is not surprising to see positive updates to  $\text{NO}_3^-$  as they depend on source and sink terms not only for  $\text{NO}_3^-$  but also for  $\text{NH}_4^+$  because of the nitrogen demand distribution scheme (Eq. 35) for plant uptake and immobilization.

730 With smaller  $k_m$ , the derivative of the substrate limiting function (Eq. 32) becomes bigger when the concentration is lower, and the off-diagonal entries in the Jacobian matrix become more dominant, increasing the probability of producing positive update. When a greater than  $[\text{NO}_3^-]$  update is produced,  $[\text{NO}_3^-]$  is expected to decrease by  $1-\alpha$  times (0.01 by default) for each subsequent iterations, making it lower than the residual concentration ( $10^{-15}$ ). If the  $\lambda$  is not greater than  $10^{-10}$ , and the  
735 solution may be considered converged because STOL is satisfied,  $[\text{NO}_3^-]$  can be very low, much below residual concentration ( $10^{-26}$ ) in Table 6. With such low concentrations, a positive update can make the scaling factor to be less than  $10^{-10}$ . The arctic site simulation aborts at a much later time than the temperate and tropical site because the uptake and immobilization rate is much smaller in the former site.

740 A lower STOL can be used to avoid or mitigate the false convergence. With  $\text{STOL} = 10^{-12}$ , the simulations abort for  $k_m = 10^{-3}$ ,  $10^{-6}$ , and  $10^{-9} \text{ mol m}^{-3}$  for the three sites due to too big an update for the diagnostic variables (PlantN, DeniN, or N<sub>2</sub>Od, Table 6). For each time step, these concentrations start with  $10^{-10}$ ; with an update as big as  $10^{-6}$ , the concentration can be lowered in several iterations using Eq. (20) to be below  $10^{-10}$  times the update, resulting too small a scaling  
745 factor. Removing the contribution of the derivatives to entries for these diagnostic species in the Jacobian can mitigate this stability and accuracy issue but may slow down the convergence or cause numerical errors. Increasing the reset value from  $10^{-10}$  can mitigate the issue. However, as long as there is a very low concentration for any species, there is a possibility for this issue to occur.

Instead of aborting the run when the scaling factor is less than the minimum allowable value  $\lambda_{min}$ ,  
750 an alternative is to consider the iteration diverges and return to the time stepping subroutine to cut time step size to increase accuracy. This mitigates the stability and accuracy challenge at the expense of computing time. Our results show the default  $\lambda_{min} = 10^{-10}$  can result in excessive error even when STOL is extremely small. It is not clear how large a  $\lambda_{min}$  value can insure accuracy without introducing unnecessary computing time. For this reason, we caution against use of SU.

755 Similar to SU, the simulations using LT run to conclusion for  $k_m = 10^{-3}, 10^{-6}$ , and  $10^{-9}$  mol m<sup>-3</sup> but abort for  $k_m = 10^{-12}$  for all of the three sites. The runs abort at 21.6, 2.46, and 1.1 year for the arctic, temperate, and tropical site because the number of time step cuts for one time step exceeds MAX\_CUT = 16 (default). Increasing MAX\_CUT to 50, the simulations run to conclusion with longer computing time (Table 5). Looking into the reason for time step cuts, it usually involves  
760 iteration with NO<sub>3</sub><sup>-</sup> concentration oscillation between the first order and zero order (Fig. 3b, for example, between  $1.69 \times 10^{-11}$  and  $1.14 \times 10^{-13}$  in the sixth layer in 0.5 year for BR-Cax site). While requiring an excessively large MAX\_CUT, all of the simulations conclude with less than a 20% increase of computing time for  $k_m$  of  $10^{-12}$  over  $10^{-9}$ . These results suggest that log transformation together with downregulation with reasonable half saturation and residual concentration can provide  
765 accurate, stable, and efficient solutions for CLM-PFLOTTRAN biogeochemistry simulations.

## 5 Summary and Conclusions

We implement CLM biogeochemistry, specifically, CLM-CN decomposition, nitrification, denitrification, and plant nitrogen uptake reactions in CLM-PFLOTTRAN. As CLM uses explicit time stepping (forward difference) and demand-based competition, the concentration is always nonnegative.  
770 PFLOTTRAN uses implicit time stepping (backward difference) and Newton-Raphson method; the concentration can become negative, which is not physical, may cause numerical instability, and introduce numerical error.

Both scaling back update in each iteration and log transformation can enforce nonnegativity. SU allows large time step sizes to achieve efficiency, but may introduce excessive numerical error if  
775 the scaling factor is small and the iterations are considered converged due to small updates. Log transformation involves multiplication of the Jacobian matrix by the concentration vector, decreasing the condition number by orders of magnitude as the concentration can be low. As a result, LT often decreases the time step size and increases computational cost. Neither SU nor LT prevents too small or 0 concentrations. When the concentration becomes too small and essentially 0, SU may stop all  
780 reactions by a small positivity update caused by consumption, numerical overshoot, or truncation error and LT can fail due to too stiff or singular Jacobian matrix. Both SU and LT require that the limitation of reactant availability on reaction rates to be represented such that solution to the mathematical representation does not introduce negative or 0 concentrations.

The first-order rate accounts for limitation of the reactant availability on the reaction rate, and  
785 the solution is nonnegative. Adding a residual concentration makes it positive. For the zero-order  
rate (or when the rate is not a function of a reactant), the Monod substrate limiting function pro-  
vides a smooth transition from a zero order when the reactant is abundant to a first order when the  
reactant becomes limiting. The downregulation relaxes with decreasing half saturation and residual  
concentration and disappears when both are 0.

790 Our CLM-PFLOTRAN spin-up simulation at an arctic, temperate, and tropical site indicates that  
accurate and stable solution can be achieved with log transformation with two to three times the  
computing time of CLM4.5 for a range of half saturation values from  $10^{-3}$  to  $10^{-9}$  and a residual  
concentration of  $10^{-15}$  for nitrogen. With half saturation of  $10^{-12}$ , the number of maximum time  
795 cuts has to be increased from the default 16 to accommodate for small time step sizes to resolve  
small concentration changes in the transition of zero and first-order rate. The computing time in-  
crease from the half saturation of  $10^{-12}$  to  $10^{-9}$  is less than 20%. As physical half saturation ranges  
from  $10^{-5}$  to  $10^{-6}$  M for nitrogen, and the detection limits are often above  $10^{-9}$  M, log trans-  
formation together with downregulation by reasonable half saturation and residual concentration is  
expected to provide an accurate, stable, and efficient solution for CLM-PFLOTRAN implementation  
800 for current CLM biogeochemistry. As more substrate limiting processes, such as labile C, P, O<sub>2</sub>, and  
H<sub>2</sub>, are implemented with lower half saturation and residual concentration, and more complicated  
rate relationship, the maximum allowable time step cut may need to be increased, and the computing  
time is expected to increase.

## 6 Code availability

805 PFLOTRAN is an open-source software. It is distributed under the terms of the GNU Lesser General  
Public License as published by the Free Software Foundation either version 2.1 of the License, or  
any later version. It is available at <https://bitbucket.org/pfotran>. Revision xxx is used for this work.

CLM-PFLOTRAN is .... Revision xxx is used for this work.

*Acknowledgements.* This research was funded by the U.S. Department of Energy, Office of Sciences, Bi-  
810 logical and Environmental Research, Terrestrial Ecosystem Sciences and Subsurface Biogeochemical Re-  
search Program, and is a product of the Next-Generation Ecosystem Experiments in the Arctic (NGEE-Arctic)  
project. ORNL is managed by UT-Battelle, LLC, for the U.S. Department of Energy under contract DE-AC05-  
00OR22725.

## References

- 815 Antonelli, L., Briani, M., D'Ambra, P., and Fraioli, V.: Positivity Issues in Adaptive Solutions of Detailed  
Chemical Schemes for Engine Simulations, in: Communications to SIMAI Congress, vol. 3, pp. 303.1–  
303.12, 2009.
- Bethke, C. M.: Geochemical and biogeochemical reaction modeling, Cambridge University Press, 2007.
- Bonan, G. B., Hartman, M. D., Parton, W. J., and Wieder, W. R.: Evaluating litter decomposition in earth  
820 system models with long-term litterbag experiments: an example using the Community Land Model ver-  
sion 4 (CLM4), *Global Change Biology*, pp. 957–974, doi:10.1111/gcb.12031, <http://dx.doi.org/10.1111/gcb.12031>, 2012.
- Boyer, E. W., Alexander, R. B., Parton, W. J., Li, C., Butterbach-Bahl, K., Donner, S. D., Skaggs, R. W.,  
and Gross, S. J. D.: Modeling Denitrification In Terrestrial And Aquatic Ecosystems At Regional  
825 Scales, *Ecological Applications*, 16, 2123–2142, doi:10.1890/1051-0761(2006)016, [http://dx.doi.org/10.1890/1051-0761\(2006\)016](http://dx.doi.org/10.1890/1051-0761(2006)016), 2006.
- Broekhuizen, N., Rickard, G. J., Bruggeman, J., and Meister, A.: An improved and generalized second order,  
unconditionally positive, mass conserving integration scheme for biochemical systems, *Applied Numer-  
ical Mathematics*, 58, 319–340, doi:10.1016/j.apnum.2006.12.002, <http://www.sciencedirect.com/science/article/pii/S0168927406002224>, 2008.
- Bruggeman, J., Burchard, H., Kooi, B. W., and Sommeijer, B.: A second-order, unconditionally  
positive, mass-conserving integration scheme for biochemical systems, *Applied Numerical Math-  
ematics*, 57, 36–58, doi:10.1016/j.apnum.2005.12.001, <http://www.sciencedirect.com/science/article/pii/S0168927405002242>, 2007.
- 830 Burchard, H., Deleersnijder, E., and Meister, A.: A high-order conservative Patankar-type dis-  
cretisation for stiff systems of production–destruction equations, *Applied Numerical Mathemat-  
ics*, 47, 1–30, doi:10.1016/S0168-9274(03)00101-6, <http://www.sciencedirect.com/science/article/pii/S0168927403001016>, 2003.
- Burchard, H., Deleersnijder, E., and Meister, A.: Application of modified Patankar schemes to stiff bioge-  
840 chemical models for the water column, *Ocean Dynamics*, 55, 326–337, doi:10.1007/s10236-005-0001-x,  
<http://link.springer.com/article/10.1007%2Fs10236-005-0001-x>, 2005.
- Chapin, F., Matson, P., and Vitousek, P.: Principles of Terrestrial Ecosystem Ecology, Springer, 2011.
- Chen, D. and Plemmons, R. J.: Nonnegativity constraints in numerical analysis, in: *Symposium on the Birth of  
Numerical Analysis*, pp. 109–140, 2009.
- 845 da Costa, A. C. L., Galbraith, D., Almeida, S., Portela, B. T. T., da Costa, M., de Athaydes Silva Junior, J.,  
Braga, A. P., de Gonçalves, P. H. L., de Oliveira, A. A. R., Fisher, R., Phillips, O. L., Metcalfe, D. B., Levy,  
P., and Meir, P.: Effect of 7 yr of experimental drought on vegetation dynamics and biomass storage of  
an eastern Amazonian rainforest, *New Phytologist*, 187, 579–591, doi:10.1111/j.1469-8137.2010.03309.x,  
<http://dx.doi.org/10.1111/j.1469-8137.2010.03309.x>, 2010.
- 850 Dickinson, R. E., Berry, J. A., Bonan, G. B., Collatz, G. J., Field, C. B., Fung, I. Y., Goulden, M., Hoffmann,  
W. A., Jackson, R. B., Myneni, R., Sellers, P. J., and Shaikh, M.: Nitrogen Controls on Climate Model  
Evapotranspiration, *Journal of Climate*, 15, 278–295, doi:10.1175/1520-0442(2002)015, [http://dx.doi.org/10.1175/1520-0442\(2002\)015](http://dx.doi.org/10.1175/1520-0442(2002)015), 2002.

- Eltrop, L. and Marschner, H.: Growth and mineral nutrition of non-mycorrhizal and mycorrhizal Norway spruce (*Picea abies*) seedlings grown in semi-hydroponic sand culture, *New Phytologist*, 133, 469–478, doi:10.1111/j.1469-8137.1996.tb01914.x, <http://dx.doi.org/10.1111/j.1469-8137.1996.tb01914.x>, 1996.
- Falkengren-Grerup, U.: Interspecies differences in the preference of ammonium and nitrate in vascular plants, *Oecologia*, 102, 305–311, doi:10.1007/BF00329797, <http://dx.doi.org/10.1007/BF00329797>, 1995.
- Fang, Y., Huang, M., Liu, C., Li, H., and Leung, L. R.: A generic biogeochemical module for Earth system models: Next Generation BioGeoChemical Module (NGBGC), version 1.0, *Geosci. Model Dev.*, 6, 1977–1988, doi:10.5194/gmd-6-1977-2013, <http://www.geosci-model-dev.net/6/1977/2013>, gMD, 2013.
- Fennell, D. E. and Gossett, J. M.: Modeling the Production of and Competition for Hydrogen in a Dechlorinating Culture, *Environmental Science & Technology*, 32, 2450–2460, doi:10.1021/es980136l, <http://pubs.acs.org/doi/pdfplus/10.1021/es980136l>, 1998.
- Foulland, E., Gosselin, M., Rivkin, R. B., Vasseur, C., and Mostajir, B.: Nitrogen uptake by heterotrophic bacteria and phytoplankton in Arctic surface waters, *Journal of Plankton Research*, 29, 369–376, <http://plankt.oxfordjournals.org/content/29/4/369.abstract>, 2007.
- Gherardi, L. A., Sala, O. E., and Yahdjian, L.: Preference for different inorganic nitrogen forms among plant functional types and species of the Patagonian steppe, *Oecologia*, 173, 1075–1081, doi:10.1007/s00442-013-2687-7, <http://dx.doi.org/10.1007/s00442-013-2687-7>, 2013.
- Grant, R. F.: Modelling changes in nitrogen cycling to sustain increases in forest productivity under elevated atmospheric CO<sub>2</sub> and contrasting site conditions, *Biogeosciences*, 10, 7703–7721, doi:10.5194/bg-10-7703-2013, <http://www.biogeosciences.net/10/7703/2013>, bG, 2013.
- Hammond, G. E.: Innovative Methods for Solving Multicomponent Biogeochemical groundwater Transport on Supercomputers, Thesis, University of Illinois at Urbana-Champaign, 2003.
- Hanson, P. and Wullschleger, S.: North American Temperate Deciduous Forest Responses to Changing Precipitation Regimes, Springer Verlag, 2003.
- Hanson, P. J., Amthor, J. S., Wullschleger, S. D., Wilson, K. B., Grant, R. F., Hartley, A., Hui, D., Hunt, J. E. R., Johnson, D. W., Kimball, J. S., King, A. W., Luo, Y., McNulty, S. G., Sun, G., Thornton, P. E., Wang, S., Williams, M., Baldocchi, D. D., and Cushman, R. M.: Oak forest carbon and water simulations: model intercomparisons and evaluations against independent data, *Ecological Monographs*, 74, 443–489, doi:10.1890/03-4049, <http://www.esajournals.org/doi/pdf/10.1890/03-4049>, 2004.
- Hartman, M. D., Baron, J. S., and Ojima, D. S.: Application of a coupled ecosystem-chemical equilibrium model, DayCent-Chem, to stream and soil chemistry in a Rocky Mountain watershed, *Ecological Modelling*, 200, 493–510, doi:10.1016/j.ecolmodel.2006.09.001, <http://www.sciencedirect.com/science/article/pii/S0304380006003942>, 2007.
- Hinkel, K. M. and Nelson, F. E.: Spatial and temporal patterns of active layer thickness at Circumpolar Active Layer Monitoring (CALM) sites in northern Alaska, 1995–2000, *Journal of Geophysical Research: Atmospheres*, 108, 8168, doi:10.1029/2001JD000927, <http://dx.doi.org/10.1029/2001JD000927>, 2003.
- Hungate, R.: The rumen microbial ecosystem, *Annual Review of Ecology and Systematics*, pp. 39–66, 1975.
- HØGh-Jensen, H., Wollenweber, B., and Schjoerring, J. K.: Kinetics of nitrate and ammonium absorption and accompanying H<sup>+</sup> fluxes in roots of *Lolium perenne* L. and N<sub>2</sub>-fixing *Trifolium repens* L, *Plant, Cell & Envi-*

- ronment, 20, 1184–1192, doi:10.1046/j.1365-3040.1997.d01-145.x, <http://dx.doi.org/10.1046/j.1365-3040.1997.d01-145.x>, 1997.
- 895 Jarrell, K. F.: Extreme Oxygen Sensitivity in Methanogenic Archaeabacteria, *BioScience*, 35, 298–302, <http://bioscience.oxfordjournals.org/content/35/5/298.abstract>, 1985.
- Kamer, K., Kennison, R. L., and Fong, P.: Rates of inorganic nitrogen uptake by the estuarine green macroalgae *Enteromorpha intestinalis* and *Ulva expansa*, vol. 2003, pp. 130–141, 2001.
- Kirchman, D. L.: The uptake of inorganic nutrients by heterotrophic bacteria, *Microbial Ecology*, 28, 255–271, 900 doi:10.1007/BF00166816, <http://dx.doi.org/10.1007/BF00166816>, 1994.
- Kirchman, D. L. and Wheeler, P. A.: Uptake of ammonium and nitrate by heterotrophic bacteria and phytoplankton in the sub-Arctic Pacific, *Deep Sea Research Part I: Oceanographic Research Papers*, 45, 347–365, doi:10.1016/S0967-0637(97)00075-7, <http://www.sciencedirect.com/science/article/pii/S0967063797000757>, 1998.
- 905 Kuzyakov, Y. and Xu, X.: Competition between roots and microorganisms for nitrogen: mechanisms and ecological relevance, *New Phytologist*, 198, 656–669, doi:10.1111/nph.12235, <http://dx.doi.org/10.1111/nph.12235>, 2013.
- Lara, M. J., Villarreal, S., Johnson, D. R., Hollister, R. D., Webber, P. J., and Tweedie, C. E.: Estimated change in tundra ecosystem function near Barrow, Alaska between 1972 and 2010, *Environmental Research Letters*, 910 7, 015 507, 2012.
- Lichtner, P. C., Hammond, G. E., Lu, C., Karra, S., Bisht, G., Andre, B., Mills, R. T., and Jitu, K.: PFLO-TRAN User Manual: A Massively Parallel Reactive Flow and Transport Model for Describing Surface and Subsurface Processes, Report, 2015.
- Middelburg, J. J. and Nieuwenhuize, J.: Nitrogen uptake by heterotrophic bacteria and phytoplankton in the 915 nitrate-rich Thames estuary, *Marine Ecology Progress Series*, 203, 13–21, <http://www.int-res.com/abstracts/meps/v203/p13-21/>, 2000.
- Nollet, L. M. L. and De Gelder, L. S. P.: *Handbook of Water Analysis* (3rd Edition), CRC Press, 2013.
- Nordin, A., Höglberg, P., and Näsholm, T.: Soil nitrogen form and plant nitrogen uptake along a boreal forest productivity gradient, *Oecologia*, 129, 125–132, doi:10.1007/s004420100698, <http://dx.doi.org/10.1007/s004420100698>, 2001.
- 920 Oleson, K., Lawrence, D., Bonan, G., Levis, S., Swenson, S., Thornton, P., Bozbiyik, A., Fisher, R., Heald, C., Kluzek, E., Lamarque, J.-F., Lawrence, P., Lipscomb, W., Muszala, S., and Sacks, W.: Technical description of version 4.5 of the Community Land Model (CLM), Ncar/tn-503+str, ncar technical note, NCAR, doi:10.5065/D6RR1W7M, [http://www.cesm.ucar.edu/models/cesm1.2/clm/CLM45\\_Tech\\_Note.pdf](http://www.cesm.ucar.edu/models/cesm1.2/clm/CLM45_Tech_Note.pdf), 2013.
- Parkhurst, D. L. and Appelo, C.: User's guide to PHREEQC (Version 2): A computer program for speciation, batch-reaction, one-dimensional transport, and inverse geochemical calculations, *Water-Resources Investigations 99-4259*, USGS, 1999.
- 925 Parton, W. J., Mosier, A. R., Ojima, D. S., Valentine, D. W., Schimel, D. S., Weier, K., and Kulmala, A. E.: Generalized model for N<sub>2</sub> and N<sub>2</sub>O production from nitrification and denitrification, *Global Biogeochemical Cycles*, 10, 401–412, doi:10.1029/96GB01455, <http://dx.doi.org/10.1029/96GB01455>, 1996.
- Parton, W. J., Holland, E. A., Del Gross, S. J., Hartman, M. D., Martin, R. E., Mosier, A. R., Ojima, D. S., and Schimel, D. S.: Generalized model for NO<sub>x</sub> and N<sub>2</sub>O emissions from soils, *Journal of Geophysical Research:*

- Atmospheres, 106, 17 403–17 419, doi:10.1029/2001JD900101, <http://dx.doi.org/10.1029/2001JD900101>, 2001.
- 935 Pfautsch, S., Rennenberg, H., Bell, T. L., and Adams, M. A.: Nitrogen uptake by Eucalyptus regnans and Acacia spp. – preferences, resource overlap and energetic costs, *Tree Physiology*, 29, 389–399, <http://treephys.oxfordjournals.org/content/29/3/389.abstract>, 2009.
- Pierre, M. and Schmitt, D.: Blowup in Reaction-Diffusion Systems with Dissipation of Mass, *SIAM Review*, 42, 93–106, doi:10.1137/S0036144599359735, <http://dx.doi.org/10.1137/S0036144599359735><http://pubs.siam.org/doi/abs/10.1137/S0036144599359735>, 2000.
- 940 Powell, T. L., Galbraith, D. R., Christoffersen, B. O., Harper, A., Imbuzeiro, H. M. A., Rowland, L., Almeida, S., Brando, P. M., da Costa, A. C. L., Costa, M. H., Levine, N. M., Malhi, Y., Saleska, S. R., Sotta, E., Williams, M., Meir, P., and Moorcroft, P. R.: Confronting model predictions of carbon fluxes with measurements of Amazon forests subjected to experimental drought, *New Phytologist*, 200, 350–365, doi:10.1111/nph.12390, <http://dx.doi.org/10.1111/nph.12390>, 2013.
- 945 Schmidt, M. W. I., Torn, M. S., Abiven, S., Dittmar, T., Guggenberger, G., Janssens, I. A., Kleber, M., Kogel-Knabner, I., Lehmann, J., Manning, D. A. C., Nannipieri, P., Rasse, D. P., Weiner, S., and Trumbore, S. E.: Persistence of soil organic matter as an ecosystem property, *Nature*, 478, 49–56, <http://dx.doi.org/10.1038/nature10386>, 10.1038/nature10386, 2011.
- 950 Shampine, L. F., Thompson, S., Kierzenka, J. A., and Byrne, G. D.: Non-negative solutions of ODEs, *Applied Mathematics and Computation*, 170, 556–569, doi:<http://dx.doi.org/10.1016/j.amc.2004.12.011>, <http://www.sciencedirect.com/science/article/pii/S0096300304009683>, 2005.
- 955 Steefel, C. I., Appelo, C. A. J., Arora, B., Jacques, D., Kalbacher, T., Kolditz, O., Lagneau, V., Lichtner, P. C., Mayer, K. U., Meeussen, J. C. L., Molins, S., Moulton, D., Shao, H., Šimůnek, J., Spycher, N., Yabusaki, S. B., and Yeh, G. T.: Reactive transport codes for subsurface environmental simulation, *Computational Geosciences*, pp. 1–34, doi:10.1007/s10596-014-9443-x, <http://dx.doi.org/10.1007/s10596-014-9443-x>, 2014.
- Tang, G., Watson, D. B., Wu, W.-M., Schadt, C. W., Parker, J. C., and Brooks, S. C.: U(VI) Bioreduction with Emulsified Vegetable Oil as the Electron Donor – Model Application to a Field Test, *Environmental Science & Technology*, 47, 3218–3225, doi:10.1021/es304643h, <http://dx.doi.org/10.1021/es304643h>, 2013a.
- 960 Tang, J., Riley, W., Koven, C., and Subin, Z.: CLM4-BeTR, a generic biogeochemical transport and reaction module for CLM4: model development, evaluation, and application, *Geoscientific Model Development*, 6, 127–140, 2013b.
- Thornton, P. E. and Rosenbloom, N. A.: Ecosystem model spin-up: Estimating steady state conditions in a coupled terrestrial carbon and nitrogen cycle model, *Ecological Modelling*, 189, 965 25–48, doi:10.1016/j.ecolmodel.2005.04.008, <http://www.sciencedirect.com/science/article/pii/S0304380005001948>, 2005.
- Veuger, B., Middelburg, J. J., Boschker, H. T. S., Nieuwenhuize, J., van Rijswijk, P., Rochelle-Newall, E. J., and Navarro, N.: Microbial uptake of dissolved organic and inorganic nitrogen in Randers Fjord, *Estuarine, Coastal and Shelf Science*, 61, 507–515, doi:10.1016/j.ecss.2004.06.014, <http://www.sciencedirect.com/science/article/pii/S0272771404001593>, 2004.

- Warren, C. R. and Adams, P. R.: Uptake of nitrate, ammonium and glycine by plants of Tasmanian wet eucalypt forests, *Tree Physiology*, 27, 413–419, <http://treephys.oxfordjournals.org/content/27/3/413.abstract>, 10.1093/treephys/27.3.413, 2007.
- Xu, T., Sonnenthal, E., Spycher, N., and Pruess, K.: TOUGHREACT—A simulation program  
975 for non-isothermal multiphase reactive geochemical transport in variably saturated geologic media: Applications to geothermal injectivity and CO<sub>2</sub> geological sequestration, *Computers & Geosciences*, 32, 145–165, doi:10.1016/j.cageo.2005.06.014, <http://www.sciencedirect.com/science/article/pii/S0098300405001500>, 2006.

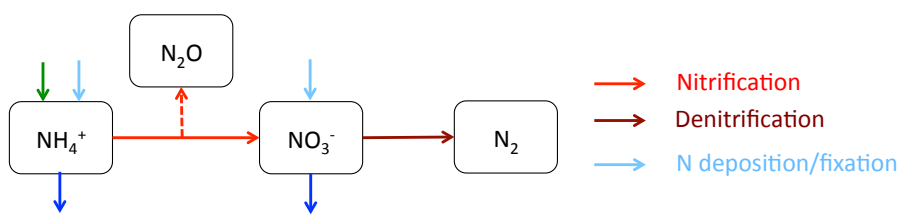
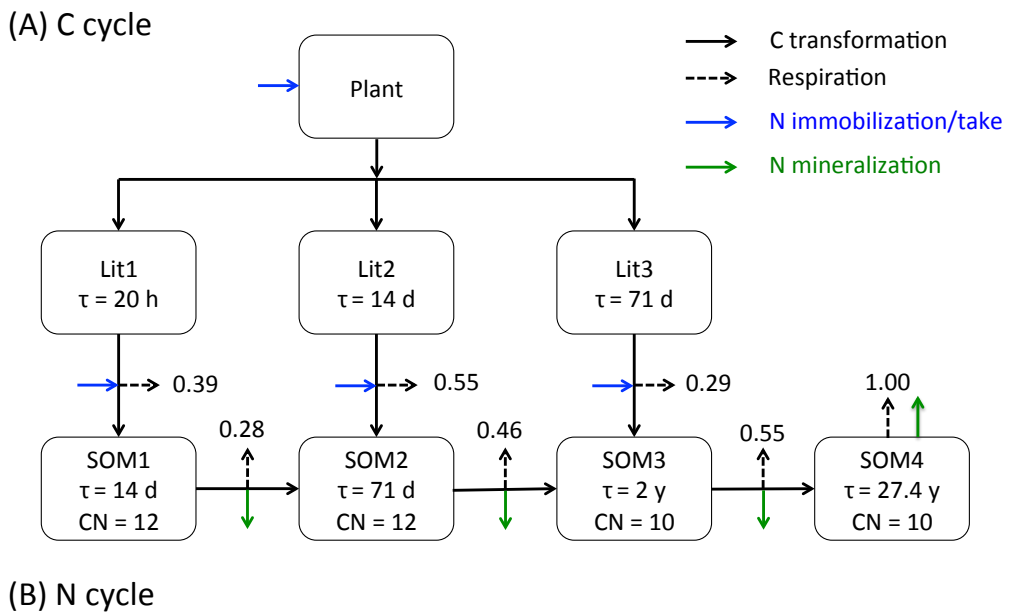


**Figure 1.** The reaction network for the carbon and nitrogen cycles implemented in this work. The carbon cycle (A) is modified from ? and ?

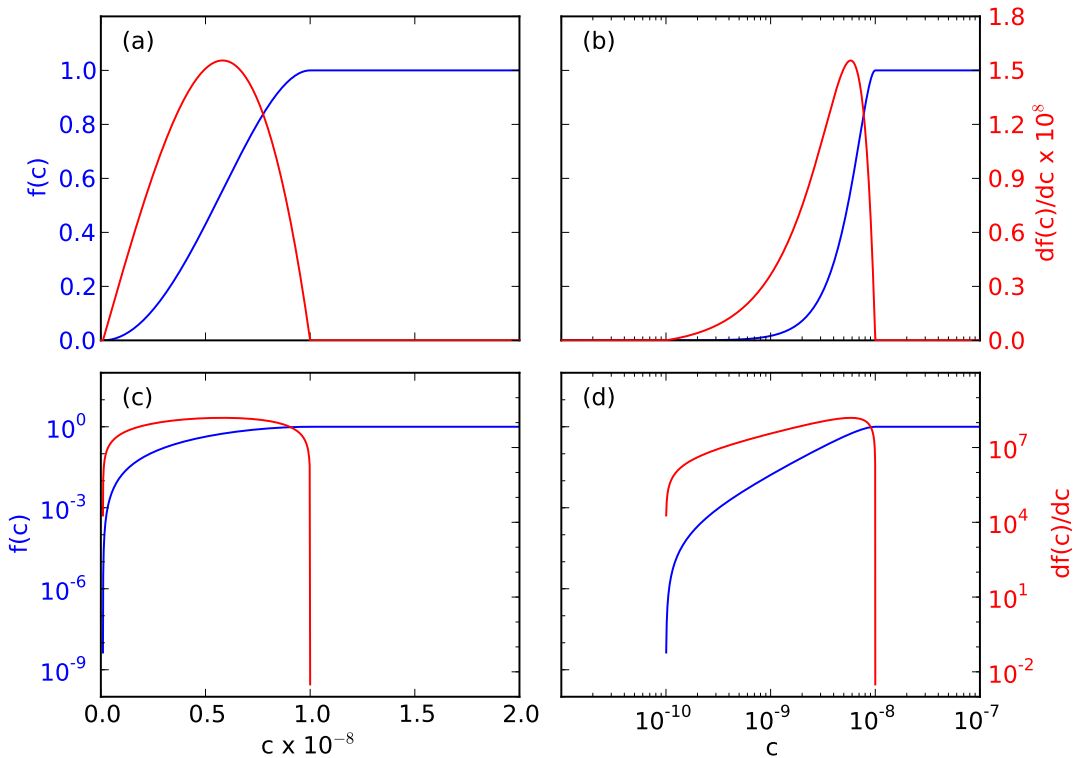


**Figure 2.** Smoothed cutoff function (Eq. 28) and derivative (Eq. 29). The y axis is in log in (c) and (d), while the x axis is in log in (b) and (d). Even though smoothed, the cutoff is a steep transition. The derivative varies by orders of magnitude in a small concentration range and requires small time step size to march through.

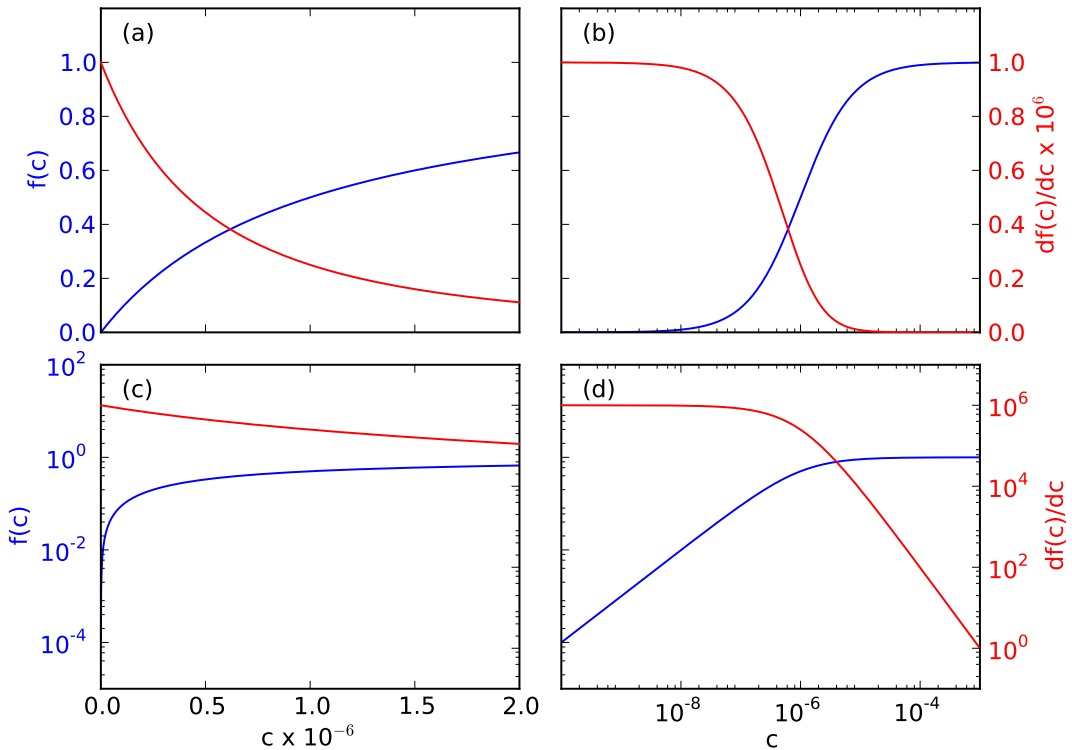


**Figure 3.** Monod substrate limiting function (Eq. 31) and derivative (Eq. 32). The y axis is in log in (c) and (d), while the x axis is in log in (b) and (d). As the function switches from zero-order to first-order, the derivative jumps six ( $k_t \text{ext m}^{-1}$ ) orders of magnitudes, requiring small time step size to step through.

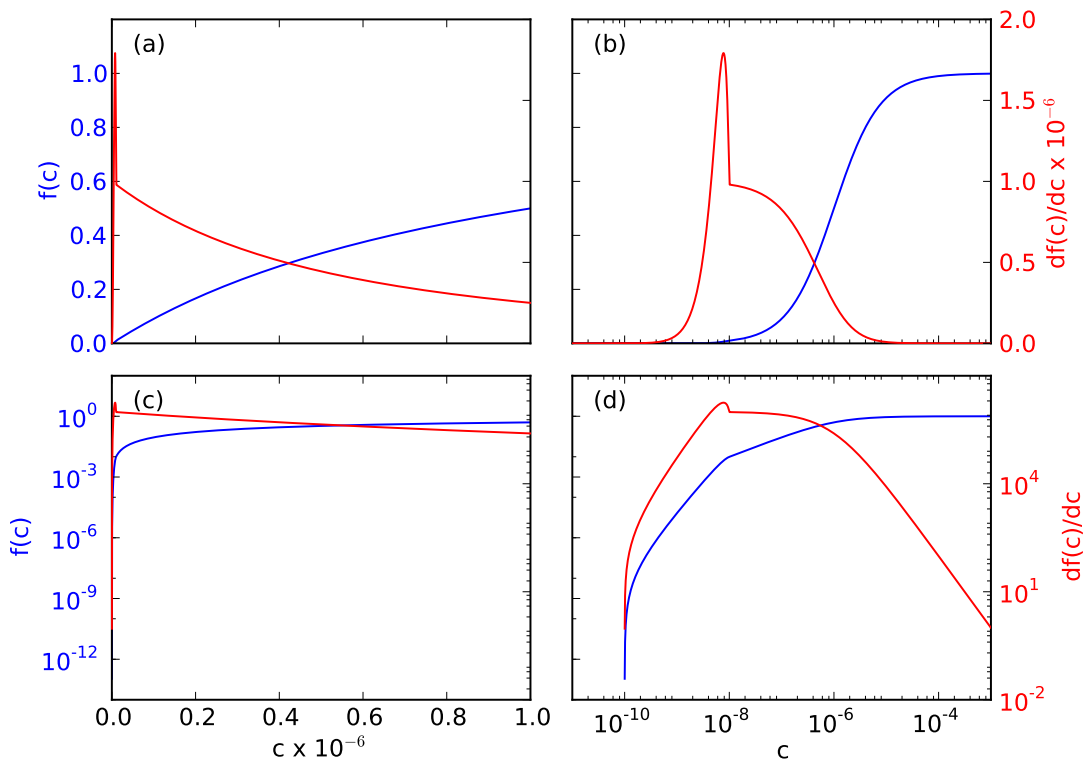


**Figure 4.** A combination of the Monod substrate limiting function (Eqs. 31 and 32, Fig. 3) and the smoothed cutoff function (Eqs. 28 and 29, Fig. 2) introduces steep transitions that require small time step sizes to march through.

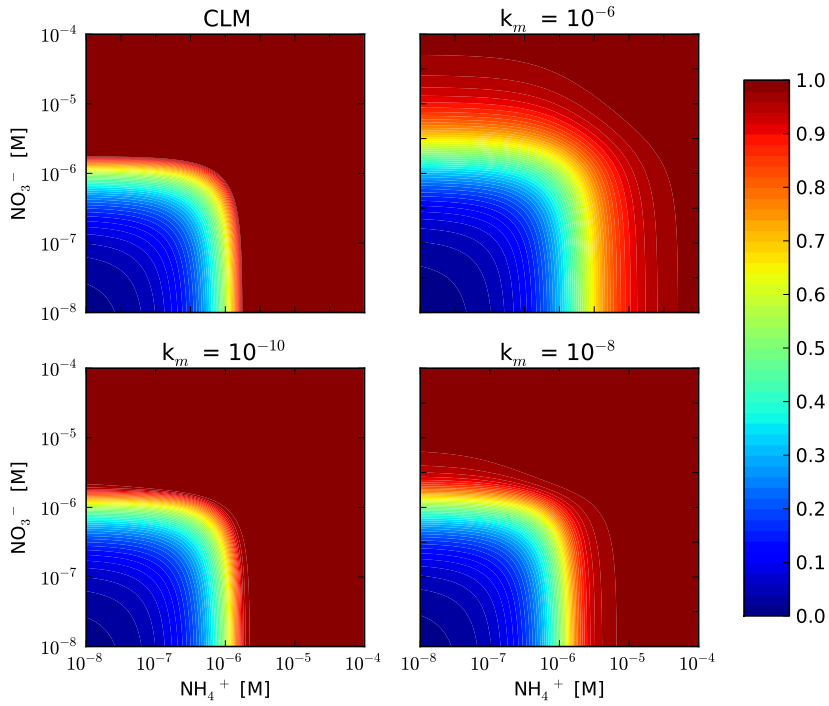


**Figure 5.** The ratio of uptake and demand ( $f_{pi}$  in Eq. 36) as a function of concentrations with CLM and representation by Eqs. (34 and 35) in a 0.5 h time step with an uptake rate of  $10^{-9} \text{ M s}^{-1}$ .  $f_{pi}$  for the new representation is less than or equal to that for CLM. The difference decreases with decreasing half saturation  $k_m$ .

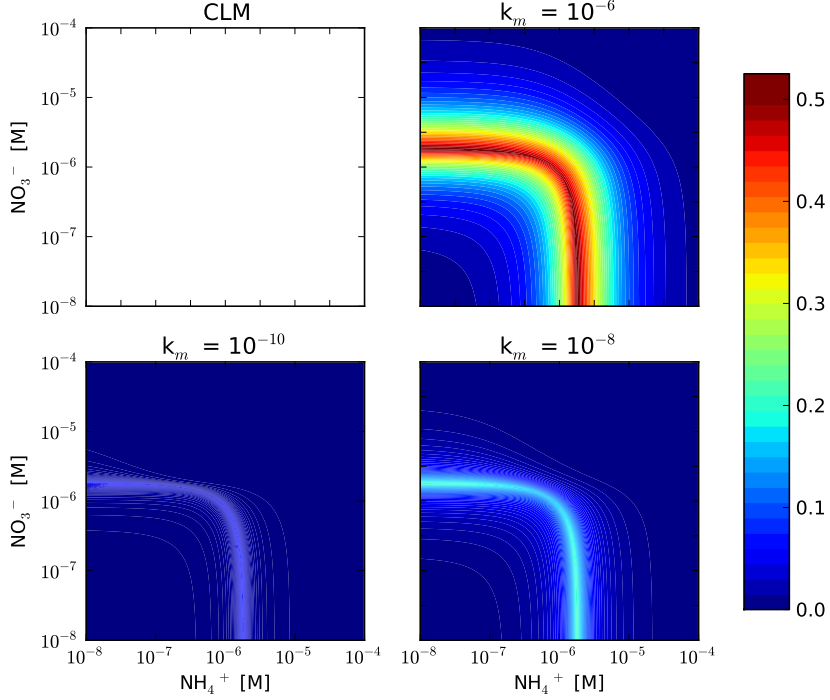


**Figure 6.** The difference plots for Fig. (5).

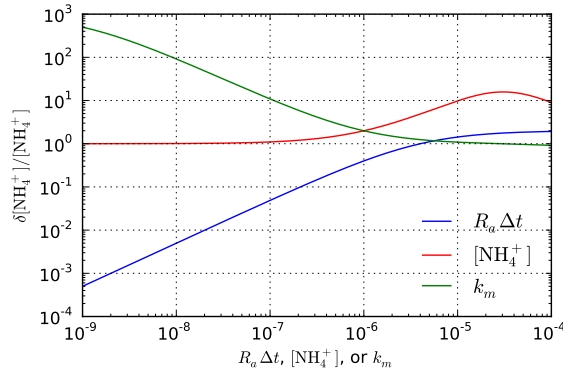


**Figure 7.** The calculated ratio of update over concentration for the first iteration as a function of time step size ( $R_a \Delta t$ ), initial concentration ( $\text{NH}_4^+$ ), and half saturation ( $k_m$ ) for solving  $d[\text{NH}_4^+]/dt = -R_a [\text{NH}_4^+]/(\text{NH}_4^+ + k_m)$  using the backward difference and Newton-Raphson method. Without scaling back the update ( $\delta$ ), the concentration in the first iteration step ( $[\text{NH}_4^+]^{k+1,1}$ ) can go negative if  $R_a \Delta t > 10^{-5}$ ,  $[\text{NH}_4^+]^k > 10^{-6}$ , or  $k_m < 10^{-6}$ . Unless specified in the figure, the base case parameters are  $R_a \Delta t = 10^{-3}$ ,  $\text{NH}_4^+ = 10^{-6}$ , and  $k_m = 10^{-6}$ .

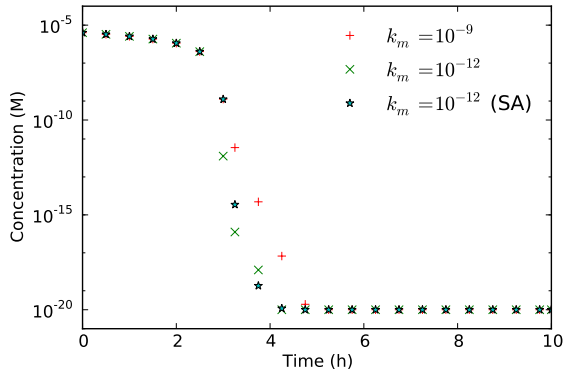


**Figure 8.** Influence of half saturation ( $k_m$ ) on the simulated  $\text{NH}_4^+$  concentration decrease due to plant uptake. Too small a half saturation may result in false convergence due to too small an update (scaling factor) during the iteration. The semi-analytical (SA) solution (Eq. 41) is used for comparison.

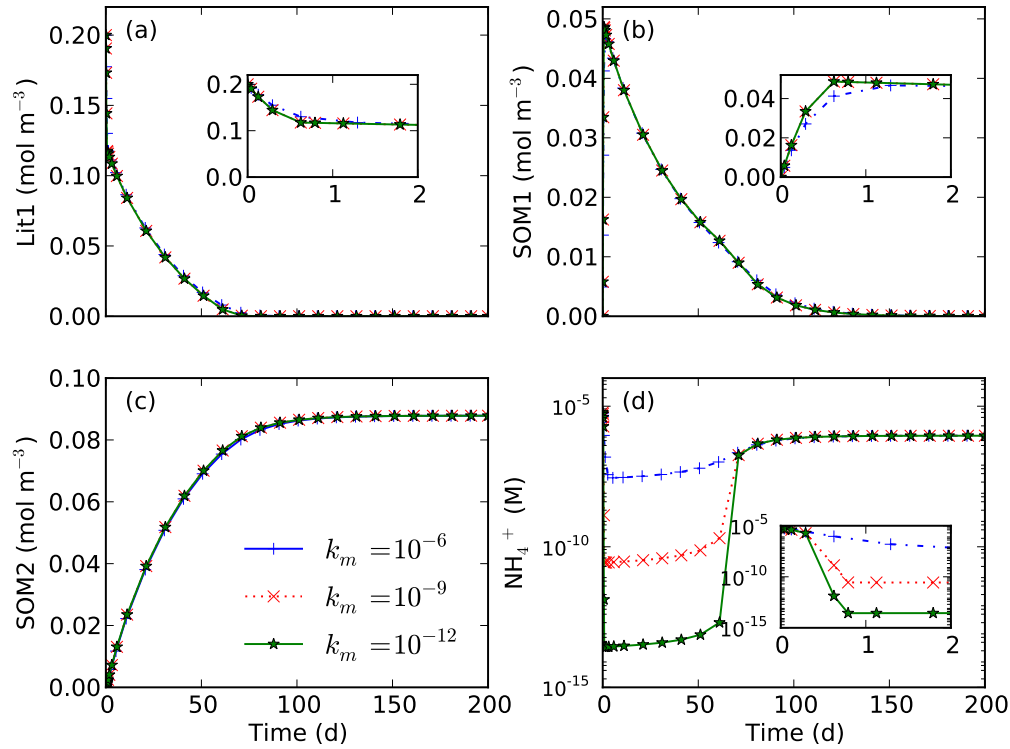


**Figure 9.** Influence of half saturation  $k_m$  on decomposition that involves both nitrogen immobilization and mineralization. Smaller half saturation can result in lower nitrogen concentration (d) but does not substantially impact the calculated concentrations other than  $\text{NH}_4^+$  (a,b,c).

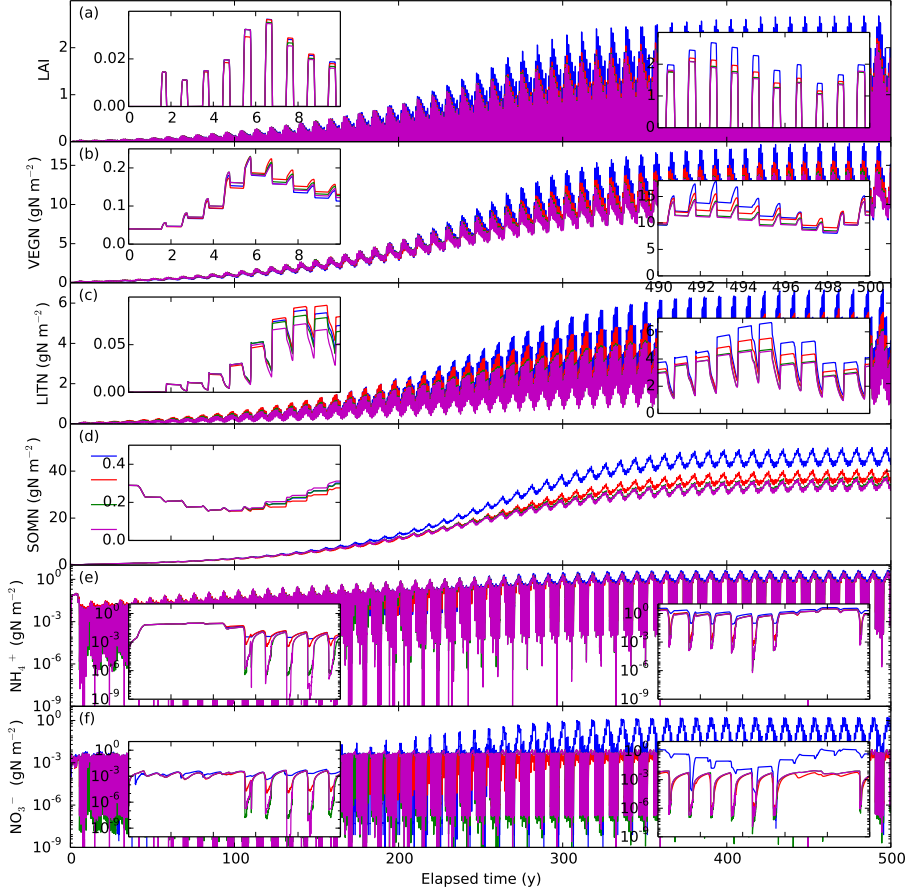


**Figure 10.** Calculated LAI and nitrogen distribution among vegetation, litter, SOM,  $\text{NH}_4^+$ , and  $\text{NO}_3^-$  pools in spin-up simulations for the US-Brw site. Log transformation is used to enforce nonnegativity for CLM-PFLOTTRAN.

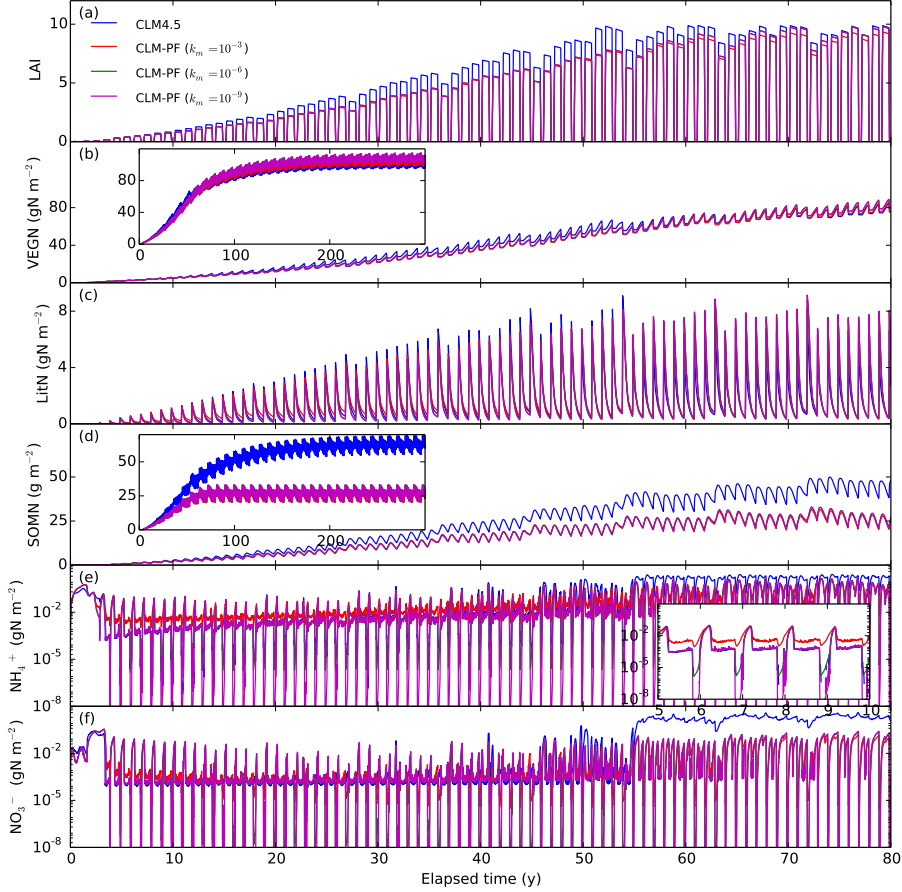


**Figure 11.** Calculated LAI and nitrogen distribution among vegetation, litter, SOM,  $\text{NH}_4^+$ , and  $\text{NO}_3^-$  pools in spin-up simulations for US-WBW site. Log transformation is used to enforce nonnegativity for CLM-PFLTRAN calculations.

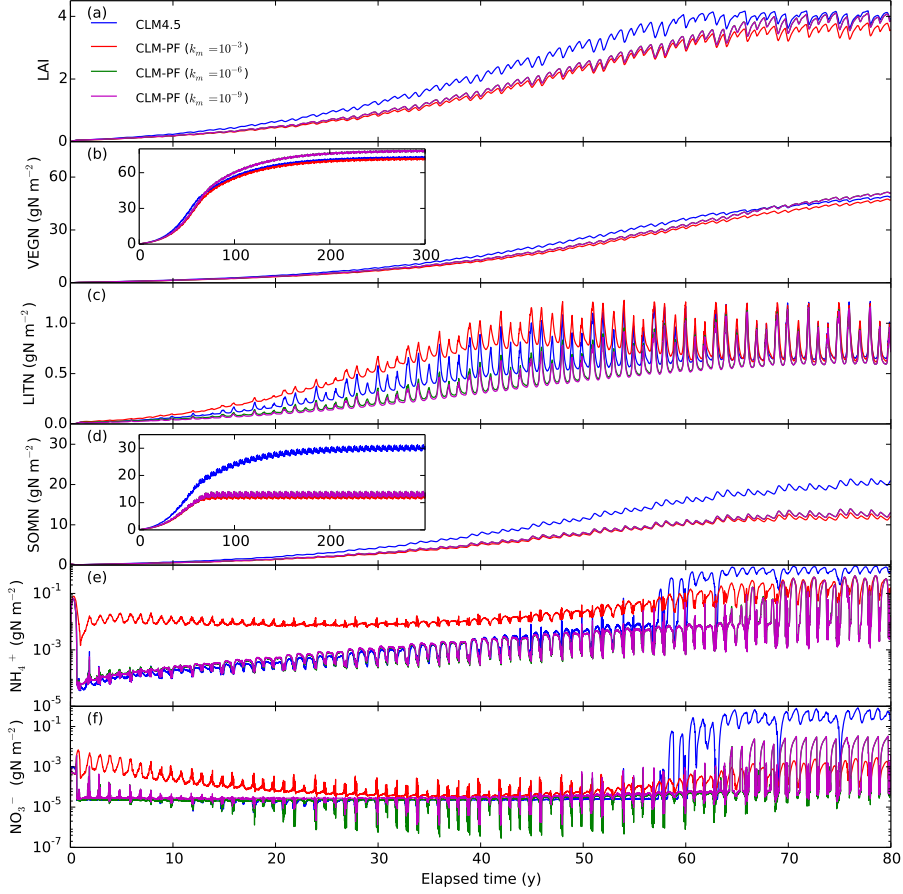


**Figure 12.** Calculated LAI and nitrogen distribution among vegetation, litter, SOM,  $\text{NH}_4^+$ , and  $\text{NO}_3^-$  pools in spin-up simulations for BR-Cax site. Log transformation is used to enforce nonnegativity for CLM-PFLOTRAN calculations.

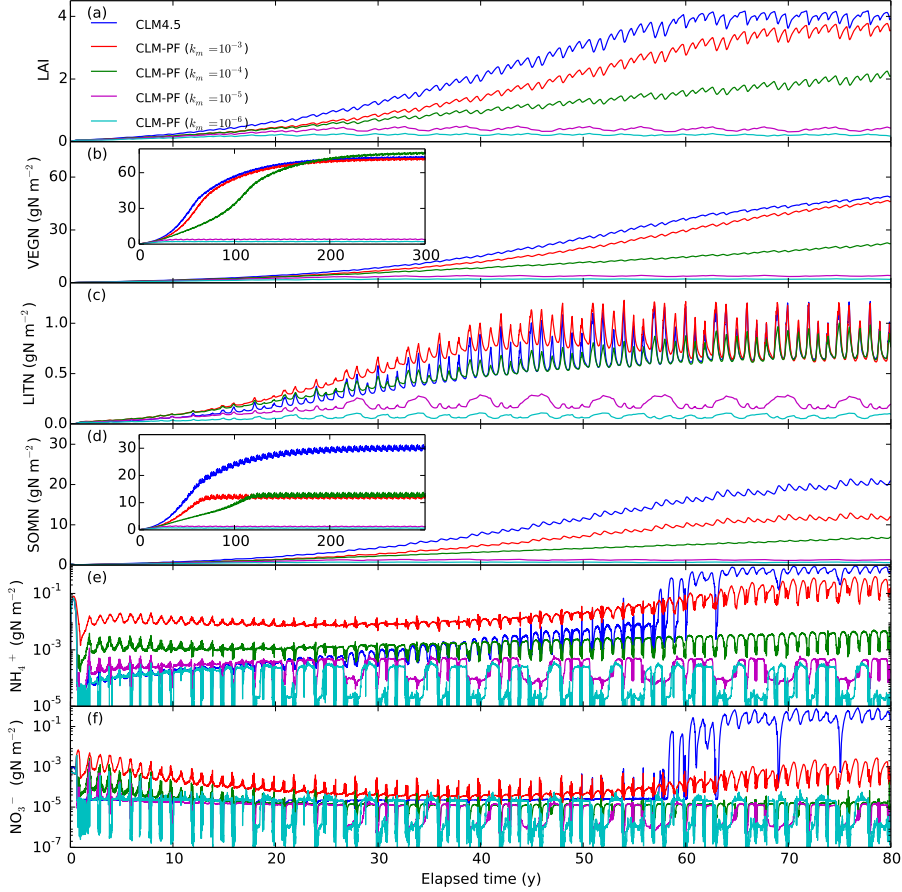


**Figure 13.** Calculated LAI and nitrogen distribution among vegetation, litter, SOM,  $\text{NH}_4^+$ , and  $\text{NO}_3^-$  pools in spin-up simulations for BR-Cax site. Scaling back update in each iteration is used enforce nonnegativity for CLM-PFLOTTRAN.

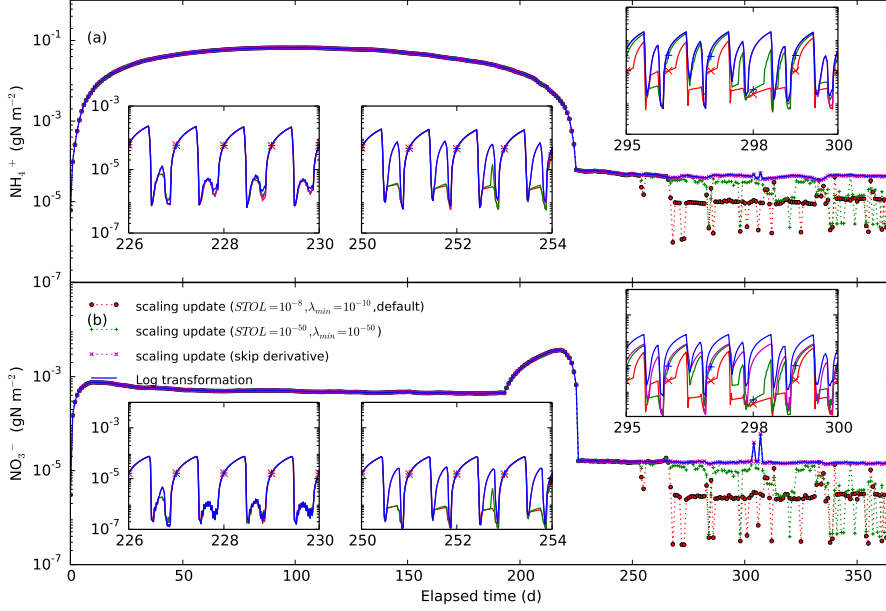


**Figure 14.** Calculated  $\text{NH}_4^+$  and  $\text{NO}_3^-$  concentration in the first year using SU (scaling update) vs. LT (log transformation) in the spin-up simulation for BR-Cax site with  $k_m = 10^{-6} \text{ mol m}^{-3}$ . “skip derivative” refers to not including the derivatives for the reaction (R11) with rate (Eq. 37) in the entries for  $\text{N}_2\text{Od}$  in the Jacobian matrix.

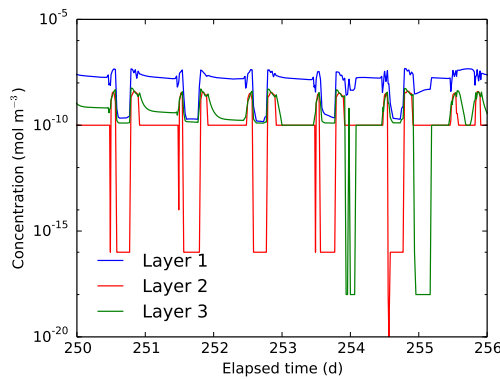


**Figure 15.** Diagnostic  $\text{N}_2\text{O}$  concentration ( $\text{N}_2\text{Od}$  from nitrification associated with net nitrogen mineralization Reaction R11 and rate Eq. 4) in the spin-up simulation for the BR-Cax site with  $k_m = 10^{-6} \text{ mol m}^{-3}$ . The concentration is reset to  $10^{-10}$  at the beginning of each CLM half hour time step. Scaling back update in each iteration is used to enforce nonnegativity.

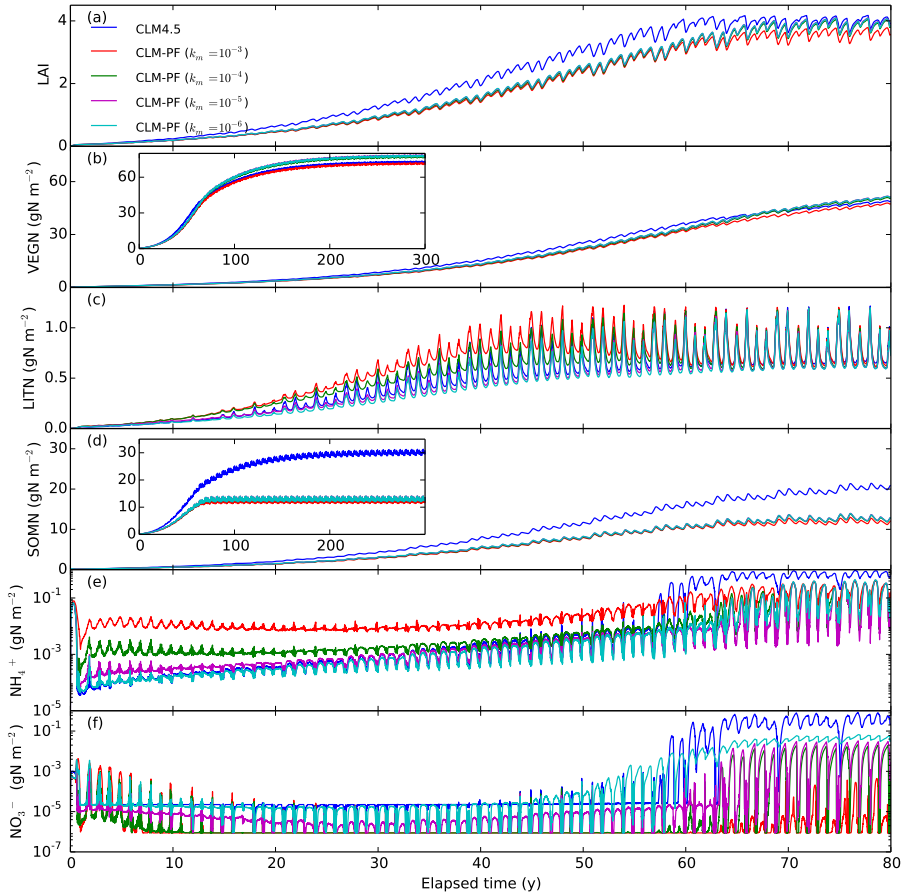


**Figure 16.** Calculated LAI and nitrogen distribution among vegetation, litter, SOM,  $\text{NH}_4^+$ , and  $\text{NO}_3^-$  pools in spin-up simulations for BR-Cax site using the CLM demand based competition for consumption downregulation, and log transformation to enforce nonnegativity.

**Table 1.** Iterations in solving  $dc/dt = -R_a c/(c+k_m)$  using backward difference and Newton Raphson method for one time step  $R_a \Delta t = 0.001$  with initial  $c = 10^{-3}$  and  $k_m = 10^{-6}$

Iteration	c	$c/(k_m+c)$	$s/(c+k_m)^2$	Residual	Jacobian	$\delta$
1	0.001	9.99E-01	9.98E-01	9.99E-01	1.00E+03	0.000998005
2	1.99501E-06	6.66E-01	1.11E+05	-3.32E-01	1.12E+05	-2.95065E-06
3	4.94566E-06	8.32E-01	2.83E+04	-1.63E-01	2.93E+04	-5.57379E-06
4	1.05195E-05	9.13E-01	7.54E+03	-7.63E-02	8.54E+03	-8.93755E-06
5	1.9457E-05	9.51E-01	2.39E+03	-2.94E-02	3.39E+03	-8.68139E-06
6	2.81384E-05	9.66E-01	1.18E+03	-6.18E-03	2.18E+03	-2.838E-06
7	3.09764E-05	9.69E-01	9.78E+02	-2.97E-04	1.98E+03	-1.49981E-07
8	3.11264E-05	9.69E-01	9.69E+02	-6.85E-07	1.97E+03	-3.47801E-10
9	3.11267E-05	9.69E-01	9.69E+02	-3.65E-12	1.97E+03	-1.85288E-15
10	3.11267E-05	9.69E-01	9.69E+02	0	1.97E+03	0

**Table 2.** Iterations in solving  $dc/dt = -R_a c/(c+k_m)$  using backward difference and Newton Raphson method for one time step  $R_a \Delta t = 0.002$  with initial  $c = 10^{-3}$  and  $k_m = 10^{-6}$  (without scaling back  $\delta$ )

Iteration	c	$c/(k_m+c)$	$s/(c+k_m)^2$	Residual	Jacobian	$\delta$
1	0.001	9.99E-01	9.98E-01	9.99E-01	5.01E+02	0.001994022
2	-0.000994022	1.00E+00	1.01E+00	4.00E-03	5.01E+02	7.97596E-06
3	-0.001001998	1.00E+00	9.98E-01	6.44E-08	5.01E+02	1.28641E-10
4	-0.001001998	1.00E+00	9.98E-01	0.00E+00	5.01E+02	0

**Table 3.** Iterations in solving  $dc/dt = -R_a c/(c+k_m)$  using backward difference and Newton Raphson method for one time step  $R_a \Delta t = 0.002$  with initial  $c = 10^{-3}$ ,  $k_m = 10^{-6}$ , and  $\alpha = 0.9999$  for scaling back  $\delta$

Iteration	c	$c/(k_m+c)$	$s/(c+k_m)^2$	Residual	Jacobian	$\delta$	$\lambda$
1	0.001	9.99E-01	9.98E-01	9.99E-01	5.01E+02	0.001994022	0.5
2	1E-07	9.09E-02	8.26E+05	-4.09E-01	8.27E+05	-4.9464E-07	1
3	5.9464E-07	3.73E-01	3.93E+05	-1.27E-01	3.94E+05	-3.22036E-07	1
4	9.16676E-07	4.78E-01	2.72E+05	-2.13E-02	2.73E+05	-7.80252E-08	1
5	9.94701E-07	4.99E-01	2.51E+05	-8.31E-04	2.52E+05	-3.29904E-09	1
6	9.98001E-07	4.99E-01	2.51E+05	-1.37E-06	2.51E+05	-5.45442E-12	1
7	9.98006E-07	5.00E-01	2.50E+05	-3.73E-12	2.51E+05	-1.48611E-17	1
8	9.98006E-07	5.00E-01	2.50E+05	0	2.51E+05	0	1

**Table 4.** Iterations in solving  $dc/dt = -R_a c/(c+k_m)$  using backward difference and Newton Raphson method for one time step  $R_a \Delta t = 0.002$  with initial  $c = 10^{-3}$  and  $k_m = 10^{-6}$  and with log transformation

Iteration	c	$c/(k_m+c)$	$s/(c+k_m)^2$	Residual	Jacobian	$\delta$
1	0.001	9.99E-01	9.98E-01	9.99E-01	5.01E-01	1.994021918
2	0.000136147	9.93E-01	5.32E+01	5.61E-01	7.53E-02	7.446148992
3	7.94668E-08	7.36E-02	8.58E+05	-4.26E-01	6.82E-02	-6.247977459
4	4.10817E-05	9.76E-01	5.65E+02	4.97E-01	4.37E-02	11.35765187
5	4.79825E-10	4.80E-04	9.99E+05	-5.00E-01	4.80E-04	-1041.52556

**Table 5.** Wall time (hour) for spin-up simulation at the arctic, temperate, and tropical sites on OIC

Site	CLM	SU ( $10^{-3}$ )	SU ( $10^{-6}$ )	SU ( $10^{-9}$ )	LT ( $10^{-3}$ )	LT ( $10^{-6}$ )	LT ( $10^{-9}$ )	LT ( $10^{-12}$ )
DC								
US-Brw	18.1	24.8	25.5	29.2	38.5	40.8	47.0	49.5
US-Pit	11.7	17.1	14.8	14.9	30.0	37.5	40.2	43.1
BR-Cax	10.9	16.2	18.6	18.0	40.2	40.5	45.7	52.0
DR								
US-Brw	18.1	21.5	21.5		35.8	35.9		
US-Pit	11.7	14.1	14.1		26.9	26.7		
BR-Cax	10.9	16.4	16.4		42.2	41.6		

SU = scaling update, LT = log transformation,  $10^{-3}$ ,  $10^{-6}$ , and  $10^{-9}$  are  $k_m$ , DC and DR = downregulating consumption as a function of concentration and rate, OIC = ORNL Institutional Cluster (Phase5), US-Brw simulation duration = 500 year and US-Pit and BR-Cax simulation duration = 300 year. For the last column LT ( $10^{-12}$ ), MAX\_CUT is increased from default 16 to 50.

**Table 6.** CLM-PFLOTRAN simulation termination before conclusion using scaling back update in iteration

Site	$k_m$	year	species	concentration	update	layer
$STOL = 10^{-8}$						
US-Brw	$10^{-12}$	346.66	$NO_3^-$	$1.26 \times 10^{-26}$	$8.20 \times 10^{-15}$	4
US-Pit	$10^{-12}$	3.56	$NO_3^-$	$2.67 \times 10^{-26}$	$2.49 \times 10^{-14}$	8
BR-Cax	$10^{-12}$	3.18	$NO_3^-$	$2.54 \times 10^{-26}$	$5.72 \times 10^{-14}$	8
$STOL = 10^{-12}$						
US-Brw	$10^{-6}$	41.78	DeniN	$10^{-20}$	$2.31 \times 10^{-10}$	2
US-Brw	$10^{-9}$	5.56	PlantN	$6.68 \times 10^{-18}$	$8.12 \times 10^{-8}$	2
US-PIT	$10^{-3}$	7.81	$N_2Od$	$10^{-20}$	$1.74 \times 10^{-9}$	1
US-PIT	$10^{-6}$	2.40	PlantN	$10^{-18}$	$2.30 \times 10^{-6}$	1
BR-Cax	$10^{-3}$	1.59	$N_2Od$	$10^{-20}$	$1.66 \times 10^{-10}$	1
BR-Cax	$10^{-6}$	0.64	$N_2Od$	$10^{-20}$	$1.91 \times 10^{-10}$	2
BR-Cax	$10^{-9}$	0.59	PlantN	$10^{-18}$	$4.92 \times 10^{-8}$	2

## Appendix A: Downregulation of consumption as a function of rates

980 The contribution of  $n$  reactions to the rate component in the residual and Jacobian for species  $i$  are

$$\mathbf{R}(i) = \sum_{j=1}^n \mu_{ij} R_j, \quad (\text{A1})$$

and

$$\mathbf{J}(i, k) = \frac{\partial \mathbf{R}(i)}{\partial \mathbf{C}(k)} = \sum_{j=1}^n \frac{\partial(\mu_{ij} R_j)}{\partial \mathbf{C}(k)}, \quad (\text{A2})$$

985 with  $\mathbf{C}$  as the concentration vector,  $\mathbf{R}$  as the rate vector,  $\mathbf{J}$  as the component of Jacobian matrix ( $m$  by  $m$ ) that is associated with  $\mathbf{R}$ ,  $\mu_{ij}$  as stoichiometric coefficient of species  $i$  in reaction  $j$  ( $\sum_{i=1}^m \mu_{ij} \mathbf{C}(i) = 0$ ), and  $R_j$  as the rate of reaction  $j$ , a function of the activities (concentration) of the reactants, products, and environmental variables (moisture, temperature, pH, redox, etc.).

### A1 Downregulation of consumption for one species

990 Depending on whether a species  $a$  (e.g.,  $\text{NH}_4^+$ ) is a reactant ( $\mu_{aj} > 0$ ) or a product ( $\mu_{aj} < 0$ ), we divide the  $n$  reactions into a demand (subscript  $da$  for demand  $a$ ) and a supply (subscript  $sa$  for supply  $a$ ) group:

$$R_{da} = \sum_{j=1}^{n_{da}} \mu_{da,aj} R_{da,j}, \quad (\text{A3})$$

and

$$R_{sa} = \sum_{j=1}^{n_{sa}} \mu_{sa,aj} R_{sa,j}, \quad (\text{A4})$$

995 with  $n_{da}$  as the number of reactions that consume species  $a$ ,  $\mu_{da,aj}$  as the stoichiometric coefficient of species  $i$  in  $a$  consuming reaction  $j$ ,  $n_{sa}$  as the number of reactions that produce species  $a$ ,  $\mu_{sa,ij}$  as the stoichiometric coefficient of species  $i$  in a producing reaction  $j$ ,  $R_{da}$  as a consumption (demand) rate ( $\text{mol s}^{-1}$ , negative), and  $R_{sa}$  as a production (supply) rate ( $\text{mol s}^{-1}$ , positive). Therefore,

$$1000 \quad \mathbf{R}(i) = \sum_{j=1}^{n_{sa}} \mu_{sa,aj} R_{sa,j} + \sum_{j=1}^{n_{da}} \mu_{da,aj} R_{da,j} = \mathbf{R}_{sa}(i) + \mathbf{R}_{da}(i), \quad (\text{A5})$$

and

$$\mathbf{J}(i, k) = \frac{\partial \mathbf{R}(i)}{\partial \mathbf{C}(k)} = \sum_{j=1}^n \frac{\partial(\mu_{ij} R_j)}{\partial \mathbf{C}(k)} = \sum_{j=1}^{n_{sa}} \frac{\partial(\mu_{sa,ij} R_{sa,j})}{\partial \mathbf{C}(k)} + \sum_{j=1}^{n_{da}} \frac{\partial(\mu_{da,ij} R_{da,j})}{\partial \mathbf{C}(k)} = \mathbf{J}_{sa} + \mathbf{J}_{da}. \quad (\text{A6})$$

We define a downregulation factor

$$d_a = \min \left( 1, -\frac{R_{sa}\Delta t + [\mathbf{C}(a) - \epsilon]V}{R_{da}\Delta t} \right) = \min \left( 1, -\frac{s_a}{D_a} \right), \quad (\text{A7})$$

1005 with  $V$  as the bulk volume or volume of liquid water of the grid cell for species with concentration unit  $\text{mol m}^{-3}$  or M. After downregulation,

$$\mathbf{R}_a = \mathbf{R}_{sa} + d_a \mathbf{R}_{da}, \quad (\text{A8})$$

$$\mathbf{J}_a(i, k) = \frac{\partial \mathbf{R}_a(i)}{\partial \mathbf{C}(k)} = \mathbf{J}_{sa}(i, k) + d_a \mathbf{J}_{da}(i, k) + \mathbf{R}_{da}(i) \frac{\partial d_a}{\partial \mathbf{C}(k)}, \quad (\text{A9})$$

$$\frac{\partial d_a}{\partial \mathbf{C}(k)} = - \left( \frac{\partial s_a}{\partial \mathbf{C}(k)} D_a - s_a \frac{\partial D_a}{\partial \mathbf{C}(k)} \right) D_a^{-2}, \quad (\text{A10})$$

$$1010 \quad \frac{\partial s_a}{\partial \mathbf{C}(a)} = \sum_{j=1}^{n_{sa}} \frac{\partial(\mu_{sa,aj} R_{sa,j})}{\partial \mathbf{C}(a)} \Delta t + V, \quad (\text{A11})$$

$$\frac{\partial s_a}{\partial \mathbf{C}(k)} = \sum_{j=1}^{n_{sa}} \frac{\partial(\mu_{sa,kj} R_{sa,j})}{\partial \mathbf{C}(k)} \Delta t, \quad (\text{A12})$$

$$\frac{\partial D_a}{\partial \mathbf{C}(k)} = \sum_{j=1}^{n_{da}} \frac{\partial(\mu_{da,kj} R_{da,j})}{\partial \mathbf{C}(k)} \Delta t, \quad (\text{A13})$$

Implementation in PFLOTRAN involves 1) adding variables  $\mathbf{R}_{sa}$ ,  $\mathbf{R}_{da}$ , and  $\mathbf{J}_a$ , 2) accumulating the values in each reaction rate formula, and 3) conducting downregulation and adding the contribution to the global residual vector and Jacobian matrix.

## A2 Downregulation of consumption for a second species

In addition to species  $a$  (e.g.,  $\text{NH}_4^+$ ), we want to downregulate another species  $l$ , for example,  $\text{NO}_3^-$ .

The treatment is the same except for the reactions that consume species  $a$  and produce species  $l$ .

Suppose we have a nitrification reaction (R10) with rate  $R_{al}$ , and  $R'_{al} = dR_{al}/d[\text{NH}_4^+]$ . The rate 1020 and derivative are added in demand rate and derivative for  $\text{NH}_4^+$  ( $\mathbf{R}_{sa}$ ,  $\mathbf{R}_{da}$ ,  $\mathbf{J}_{sa}$ ,  $\mathbf{J}_{da}$ ), not in the sink rate and derivative for  $\text{NO}_3^-$  ( $\mathbf{R}_{sl}$ ,  $\mathbf{R}_{dl}$ ,  $\mathbf{J}_{sl}$ ,  $\mathbf{J}_{dl}$ ). Define a downregulation factor

$$d_l = \min \left( 1, -\frac{R_{sl}\Delta t + (\mathbf{C}(l) - \epsilon)V_w + \underline{R_{dl}d_a\Delta t}}{R_{dl}\Delta t} \right) = \min(1, -\frac{s_l}{D_l}), \quad (\text{A14})$$

$$\mathbf{R}_l = \mathbf{R}_{sl} + d_l \mathbf{R}_{dl}, \quad (\text{A15})$$

$$\mathbf{J}_l(i, k) = \frac{\partial \mathbf{R}_l(i)}{\partial \mathbf{C}(k)} = \mathbf{J}_{sl}(i, k) + d_l \mathbf{J}_{dl}(i, k) + \mathbf{R}_{dl}(i) \frac{\partial d_l}{\partial \mathbf{C}(k)}, \quad (\text{A16})$$

1025  $\frac{\partial d_l}{\partial \mathbf{C}(k)} = - \left( \frac{\partial s_l}{\partial \mathbf{C}(k)} D_l - s_l \frac{\partial D_l}{\partial \mathbf{C}(k)} \right) D_l^{-2}, \quad (\text{A17})$

$$\frac{\partial s_l}{\partial \mathbf{C}(l)} = \sum_{j=1}^{n_{sl}} \frac{\partial (\mu_{sl,lj} R_{sl,j})}{\partial \mathbf{C}(l)} \Delta t + V_w + \underline{\frac{\partial (R_{al} d_a)}{\partial \mathbf{C}(l)}}, \quad (\text{A18})$$

$$\frac{\partial s_l}{\partial \mathbf{C}(k)} = \sum_{j=1}^{n_{sl}} \frac{\partial (\mu_{sl,kj} R_{sl,j})}{\partial \mathbf{C}(k)} \Delta t + \underline{\frac{\partial (R_{al} d_a)}{\partial \mathbf{C}(K)}}, \quad (\text{A19})$$

and

$$\frac{\partial D_a}{\partial \mathbf{C}(k)} = \sum_{j=1}^{n_{da}} \frac{\partial (\mu_{da,kj} R_{da,j})}{\partial \mathbf{C}(k)} \Delta t. \quad (\text{A20})$$

1030 In addition to variables  $\mathbf{R}_{sl}$ ,  $\mathbf{R}_{dl}$ , and  $\mathbf{J}_l$ , downregulating the second species requires two additional variables,  $R_{al}$ , and  $R'_{al}$ . When accumulating the values in each reaction rate formula, the production rate from the reaction that consumes the first species has to be carefully treated as it is downregulated for the first species. Conducting downregulation involves additional terms, as underlined in the equations. Compared with the downregulation for the first species, downregulating the  
1035 second species that can be produced from the first species with a simple  $A \rightarrow B$  reaction becomes much more complicated. If we add another reaction that consumes the second species to produce the first species, this approach has to be modified.

In general, many if not all species need to be downregulated. Extending this approach involves adding many variables (vectors and matrices) to track the consumption and production rates and their  
1040 derivatives. The consumption and production relationship among many species can be complicated, making generalization of this approach challenging if not infeasible.